

APPENDIX 4

A STOCHASTIC/DETERMINISTIC METHODOLOGY
FOR ESTIMATING RESUSPENSION POTENTIAL AND RISK
AND ITS APPLICATION TO THE TRENCH CHANNEL OF THE DETROIT RIVER

A STOCHASTIC/DETERMINISTIC METHODOLOGY FOR ESTIMATING RESUSPENSION POTENTIAL
AND RISK AND ITS APPLICATION TO THE TRENTON CHANNEL OF THE DETROIT RIVER

An Interim Report for
the U.S. Environmental Protection Agency
Upper Great Lakes Connecting Channels Study
Project No. R005852-01

DRAFT

Prepared by

Keith W. Bedford, Ph.D.
Gregory Koltun, Onyx Wai, Charles M. Libicki, Ph.D.,
and R. Van Evra

Dept. Civil Engineering
Ohio State University
2070 Neil Avenue
Columbus, Ohio 43221

First Draft April 7, 1987
Second Draft September 20, 1987

INTRODUCTION AND OBJECTIVES

Parameterizing and measuring sediment resuspension is a most challenging scientific problem which must be reliably solved if optimal toxic substance management practices are to be identified for the Great Lakes, Connecting Channels and Areas of Concern. This scientific goal is being addressed from a number of different points of view which contain varying degrees of resolution and quite different analytical viewpoints, but are united in the fact that these methods are all recently developed, to a greater or lesser extent are untested, and most importantly, must allow estimates to be made which are valid over the long term life of the management plans.

The intent of this document is to present a procedure for estimating the resuspension potential of a region which allows forecasts to be made over such long periods of time. The level of structure in this model will provide answers required for the fate and disposal models of the type being developed for EPA Grosse Ile Laboratory by Dr. Dominic Di Toro. The method is applied in the sense that results from existing though perhaps not fully tested experiments are brought together, therefore the methodology is marked by its comprehensive amalgamation of existing data and not by any newly developed concept. Further, this method brings together the best features of both stochastic and deterministic modeling and data collection and analyses which appears to be a much more efficient use of these approaches than the usually mutually exclusive treatments. The authors fully well realize that full mechanistic analysis and modeling have been somewhat suppressed; rather this approach is presented in the spirit of being a "first cut tool" for regulation and monitoring personnel which requires readily available, operationally collected data, and results in identification of areas requiring much further and more advanced analysis.

This is an interim report based on the author's work on EPA Agreement No. R005852-01. As this project is part of the Trenton Channel, Connecting Channels work, this area becomes the first application of the method.

AN OVERVIEW OF RESUSPENSION AND ENTRAINMENT'

The Setting

Resuspension of bottom sediments is the net result of: a wide variety of different fluid mechanical processes with variability spanning more than six decades in time and space scale; particle material properties such as size distribution and composition; and bottom characteristics such as the degree of consolidation, roughness, bedforms and bioturbation. The aggregate of these effects is concentrated in a thin region adjacent to and within the bottom called the benthic boundary layer. After Bowen (1976), it is noted that within this thin layer, very strong vertical gradients in physical, chemical and biological parameters occur.

From the review article by Bedford and Abdelrhman (1987) and the works of McCave (1976), Nihoul (1977), Bowden (1978) and Nowell and Hollister (1986), Fig. 1 contains a schematic of the factors affecting the bottom boundary layer and therefore resuspension. In the sequel, this review and methodology do not address large scale geological effects such as rifts, nor very large impulsive loadings such as caused by earthquakes, water spouts or "released" ice-dams. Attention is focused on the fluid mechanical effects and those particle and small scale bottom factors affecting the prediction of entrainment.

As noted in Bedford and Abdelrhman (1987), the fluid mechanical mechanisms are quite diverse and broad band. Table 1 (after Boyce, 1974) summarizes a list of such processes. It should be emphasized that not all these phenomena exist simultaneously; indeed much of the entrainment estimate

can justifiably be done with models incorporating one or at most two monochromatic forcing functions. It is possible to group all these phenomena into four broad classes of fluid forcing functions including: (1) oscillatory motions composed of short and long period surface gravity waves and/or internal waves; 2.) steady or quasi-steady (time variation as a sequence of steady steps) currents; 3.) Coriolis effects; and 4.) turbulence resulting from current shear, separated flows and breaking waves, etc.

Definitions and Continuum Equations - Nearbottom

In order to define certain terms and as an aid to seeing what factors are being parameterized in the resuspension procedure, it is necessary to present a summary of certain key equations that govern the distribution of sediment concentration and horizontal and vertical fluxes near and at the bottom. Following Lumley (1978), the conservation of mass equation for a dilute suspension can be written for each grain size in the distribution. In this fashion, each equation would have its own particle settling velocity and source sink term for flocculation, etc. Conversely, an equation for the total sediment concentration can be derived which has a time and space varying settling velocity, i.e., a full knowledge of the grain size distribution is required. For the sake of discussion, Equation (1) can be written for the concentration of a grain size class with settling velocity w_s . Figure 2 contains the coordinate system which is referenced to a streamline coordinate (x) in the horizontal and vertical coordinate z which is perpendicular to the x coordinate and (hopefully) aligned with gravity. The overbar indicates traditional Reynolds averaging for turbulence analysis.

$$\frac{\partial \bar{c}}{\partial t} + \frac{\partial \bar{N}_x}{\partial x} + \frac{\partial \bar{N}_z}{\partial z} = \bar{s} \quad (1)$$

In these equations, the horizontal (x) and vertical (z) fluxes are defined at a point in the water columns as

$$\bar{N}_x = \bar{u} \bar{c} + \overline{u'c'} - D \frac{\partial \bar{c}}{\partial x} \quad (2)$$

and

$$\bar{N}_z = \bar{w} \bar{c} + \overline{w'c'} - w_s \bar{c} - D \frac{\partial \bar{c}}{\partial z} \quad (3)$$

where u and w are the horizontal and vertical fluid velocities in the x and y direction, respectively; w_s is the settling velocity for the particle size class; D is a coefficient accounting for transport by molecular effects; N_x and N_z , the fluxes, have units of mass per area per time ($M/L^2/t$) in the respective direction; and s is a source/sink term accounting for flocculation, coagulation, etc. The Reynolds temporal averaging is based upon the following decomposition for any variable α ;

$$\alpha = \bar{\alpha} + \alpha'$$

where
$$\bar{\alpha} = \frac{1}{T} \int_t^{t+T} \alpha dt \quad (4)$$

If Equation (3) is evaluated at the bottom, $z \approx 0$, then the time average vertical velocity, \bar{w} , is zero and the vertical flux at the bottom is

$$\bar{N}_z(x, z=0, t) = N_{z0} = \overline{w'c'} - \overline{w_s c} - D \frac{\partial \bar{c}}{\partial z} \quad (5)$$

(a.) (b.) (c.)

Term (b.) is the deposition flux (always negative), term (c.) is the molecular flux (positive or negative) and term (a) is the entrainment or resuspension flux (positive). The molecular flux term is usually considered quite small.

Relating the bottom flux \overline{Nz}_0 to the transport activity at a point not too far off the bottom is important in that both the measurement of Nz_0 and specification of Nz_0 in grid-based predictive-deterministic models requires this relation. Two procedures exist; the first is based upon an integral control volume approach; while the second is a direct numerical approximation of the derivatives in Equation (1).

If as in Figure 1 the control volume is defined as extending over dz between the bottom $z = 0$ and $z = \eta$, the integral expression Nz_0 becomes (Bedford et al., 1987a, 1987b) for a flat bottom:

$$\overline{Nz}_0 = \frac{d}{dt} \int_0^\eta \bar{c} dz + \overline{Nz}(x, z = \eta, t) + \frac{\partial \overline{Nx}}{\partial x} - \bar{S} \quad (6)$$

Equation (6) can be directly solved for entrainment

$$\begin{aligned} \overline{w^*c^*}(z=0) = & \frac{d}{dt} \int_0^\eta \bar{c} dz + \overline{Nz}(x, z = \eta, t) + w_s \bar{c}(x, z = 0, t) \\ & + \frac{\partial \overline{Nx}}{\partial x} - \bar{S} \end{aligned} \quad (7)$$

This equation is the basis for the resuspension measurements reported later on.

A second procedure involves direct approximation of the derivatives in Equation (1). Finite differences or elements are used and the heart of such a method is the presumption that the variation in the dependent variable \bar{c} is in a polynomial form. Therefore, the vertical variation of c is assumed a priori. No such assumption is necessary in Equations (6) and (7). By assuming simple centered second order approximations (quadratic polynomial variation) extending from the bottom $z=0$ to $z=\eta$, then a time and space centered second order computational approximation for Equation (1) becomes:

$$\overline{Nz}_0 = \eta \left[\frac{\partial}{\partial t} \bar{c}(x, z = \eta/2, t) + \frac{\partial \overline{Nx}}{\partial x} - \bar{S} \right] + \overline{Nz}(x, z = \eta, t) \quad (8)$$

Although somewhat similar to Equation (6), considerable differences occur particularly as regards the accumulation of error in the numerical approximation to the time and space derivatives. Again, with available data on $\bar{c}(x, z=0, t)$, $\overline{w'c'}(x, z=0, t)$ becomes:

$$\overline{w'c'}(z=0) = \eta \left[\frac{\partial \bar{c}}{\partial t} (x, z = \frac{\eta}{2}, t) + \frac{\partial \bar{N}_x}{\partial x} - \bar{S} \right] + \bar{N}_z(x, z=\eta, t) + w_s \bar{c}(x, z=0, t) \quad (9)$$

Definitions and Equations - Water Column Mass Balance

While the continuum description is useful in defining the details of resuspension and deposition at the bottom, the information on resuspension is to be employed in mass balance models of the entire water column. Such mass balance equations are conveniently formed from a control volume point of view and have been derived elsewhere in many different forms. As in the previous section, one can derive these formulae for each grain size class with a constant w_s for each class size or the equations for the mixture concentration and a time and space varying w_s can be employed.

For the Trenton Channel which is basically a river, the simplest control volume (Figure 3) would have a length Δx and extend across the width and depth of the channel at the particular cross section. Using area averaged definitions for the dependent variables, the mass balance equation for this control volume element becomes

$$\frac{\partial(CA\Delta x)}{\partial t} + \frac{\partial(UCA\Delta x)}{\partial x} + \frac{\partial}{\partial x} [KADx \frac{\partial c}{\partial x}] + S_C^* + S_E^* + S_D^* = 0 \quad (10)$$

In this equation, C is the area average mass concentration, (M/L^3); A is the cross sectional area at the middle of the control volume, (L^2); U is the cross section average velocity, (L/t); K is a coefficient incorporating turbulence effects (dispersion, diffusivity, etc.), (L^2/t); S_C^* is a source sink term accounting for creation or destruction of the grain class size due

to flocculation, coagulation, disaggregation, etc. (M/t); S_E^* is the time rate at which sediment mass is entrained into the control volume from the bottom, (M/t); and S_D^* is the time rate at which mass is eliminated from the cv by deposition, (M/t).

If as is often done for long time period calculations, the cross sectional area is assumed not to vary substantially from one time step to the next, Equation (10) can be put on an intensive basis by dividing through by the volume, V, of the cv, ($= A\Delta x$); this yields

$$\frac{\partial C}{\partial t} + \frac{\partial}{\partial x} (UC) + \frac{1}{A} \frac{\partial}{\partial x} (KA \frac{\partial C}{\partial x}) + S_C + S_E + S_D = 0 \quad (11)$$

In Equation (11), $S_C = S_C^*/V$; $S_D = S_D^*/V$; and $S_E = S_E^*/V$

As activities contributing to S_C occur within the water column and are being addressed in other research programs, no further discussion of S_C occurs. While aspects of S_D are also considered, the major focus of the rest of this report is in specification of S_E . Before discussing various hypothesized forms for S_E , it is important to see how S_E relates to \bar{N}_z (Equation 5) and terms a, b, and c. First of all as mentioned before, term c (Equ 5.) is ignored. With regard to entrainment (term a) S_E^* (Equation 10) is the time rate of change of mass injected into the cv off the bottom of the cv covered by water. If the bottom area is defined as A_B then S_E^* and term a are related as follows:

$$S_E^* = \int \int \overline{w^*c^*} dA_B \quad (12)$$

If $\overline{w^*c^*}$ is constant across the bottom, then

$$S_E^* = \overline{w^*c^*} A_B \quad (13)$$

By following the same line of reasoning, the deposition term can be evaluated. In total then:

$$S_E^* + S_D^* = \int \int \bar{N}z_0 \, dA_B = \int (\bar{w}^T \bar{c}^T - w_S \bar{c}) \, dA_B \quad (14)$$

The conversion to mass per control volume per unit time requires division by V as defined for equation (11). All these relations may also be performed for grid based control volumes such as used in two and three dimensional models. In this case, A_B becomes the bottom area of the grid cell.

Summary of Empirical/Hypothesized Parameterizations for Entrainment and Deposition

An extensive series of forms for S_E^* and S_D^* exist. From work performed for other research (Lee and Bedford, 1986), a number of forms for specifying these source sink terms have been reviewed and tabularized in Tables 2 and 3. Table 4 contains a summary of various forms suggested for calculating the settling velocity w_S . In some sense, a number of the following features are embodied in these formulae. First, entrainment is parameterized by a difference between fluid water column activity as measured by shear and a critical shear which represents the material strength of the bottom. Second, most of these formulae incorporate some measure of the degree of compaction of the bottom material. The use of deposition time for this measure by Ziegler and Lick (1986) has a number of modeling attributes. The result of these features is the necessity then of including "bottom" effects in the entrainment representation. Third, the effects of fine grain often cohesive sediments introduce complexities in both entrainment and deposition rates and their prediction although close examination of all formulae reveals deposition rates to be still primarily driven by the settling velocity w_S . Fourth, the

effects of flocculation and bioturbation are for the most part excluded. Finally, in this author's opinion, most of these formulae have never been tested with in-situ data.

For purposes of this work, the models for S_E and S_D presented in Ziegler and Lick (1986) will be used as summarized in Table 5.

RELATIONSHIP BETWEEN ENTRAINMENT/DEPOSITION AND FORCING FUNCTIONS

From the summary information in Tables 2-5, it is clear that three items are quite important in the parameterization of S_E and S_D : the grain size distribution of the suspended material; some knowledge of the bottom material conditions, i.e., degree of consolidation, shear strength, etc., and the near bottom shear stress generated by water column velocity gradients. Of critical importance to the determination of S_E^* , emphasized here, are the last two, particularly the shear stress. The shear stress acting on the bottom results, as mentioned earlier, from a variety of different and often superimposed water column processes which will be called forcing functions. Within each class of forcing function (Table 1) there may be several subsets of the same process; for instance, surface gravity waves may, as a result of storms, be freshly created in the wind direction but superimposed on swell arriving from a different direction due to a previous wind condition.

From the article by Bedford and Abdelrhman (1987) mechanistic or boundary layer formulations are available which have been partially verified for in-situ conditions and which can be used to relate the bottom shear, τ , (eqn 5.3, Table 5) to more readily measured variables such as average water column velocity or wave characteristics. Three classes of these boundary layer formulations exist for each as distinguished by the type of forcing function to be included in the estimate for shear: 1.) Steady or quasi steady

currents; 2.) oscillatory wave driven from either wind driven or internal waves; and 3) combined wave current forcing functions. While a detailed review of all the theories in these categories is beyond the report, it is possible to summarize for each of these three several prevalent methods for determining bottom shear τ or τ_b . Table 6 contains those for steady flow, Table 7 addresses wave only conditions, while Table 8 contains the combined wave/current flow shear stress procedure due to Grant (see Grant and Madsen, 1986 and Glenn and Grant, 1987). It should be noted that combined flow bottom shear is not the simple sum of steady current and wave bottom shear. Indeed, the Grant (Grant and Madsen, 1979) expressions reflect non-linear interactions which have been partially field verified (Grant et al., 1984). For steady or quasi-steady open channel flow it is also possible to derive expressions for bottom shear in terms of the average velocity or flow (Valin, 1978).

In reviewing these formulae, it is necessary to first justify or assume that that particular boundary layer solution exists in situ for the forcing functions being incorporated into τ . It is also apparent that these formulae require a measure of the temporal average velocity near the bed or the water column average velocity or flow and/or the wave characteristics including period, amplitude, and wavelength. The necessity of specifying these data is, on the one hand, an improvement in that these data are much easier to measure or estimate than the shear stress or entrainment. However, flow and wave data are directly related to atmospheric phenomena which are stochastic. An extremely difficult decision is therefore required as to which set of flow and wave conditions (i.e., what average) to use in estimating shear and in turn resuspension. Indeed, there is extreme variability in the flow and wave conditions which varies from day to day and season to season. As it is not possible to simulate all the possible resuspension conditions in deterministic

models and since it is also not possible to measure resuspension for all possible types of forcing function conditions, it appears necessary to recast this problem by consideration of a probabilistic/stochastic approach.

PROBABILISTIC WATER COLUMN SEDIMENT MASS BALANCE MODEL

A stochastic/probabilistic or conjunctive framework for calculating expected average water column concentrations of toxics and their variance has been developed by DiToro et al., 1985, and as the entrainment estimation procedure meshes with it, the method is briefly summarized as adapted to the case of sediment transport.

If a waterway such as the Trenton Channel is segmented into a sequence of control volumes (each extending across the channel so the one dimensional case applies) then a mass balance equation for each control volume can be written in vector matrix form for a grain size class concentration, c ,

$$\frac{dc}{dt} = - \underline{A} c + S_E(t) \quad (15)$$

where \underline{A} is a square matrix of transfer coefficients resulting from discretizing the advection and dispersion terms, settling of material out of control volume, and inclusion of all bio-chemical first-order reaction rates that may result in the creation or destruction of mass within the class size. Flocculation and aggregation are ignored at this time. $S_E(t)$ is the entrainment source/source column vector with each entry representing the resuspension input from the individual control volumes. The entries in $S_E(t)$ are related to Equations (10), (11), and (12) in that for a system of N control volumes, each with its own volume V

$$S_E(t) = \left[S_E^* / V_1, S_E^* / V_2, \dots, S_E^* / V_N \right]^T \quad (16)$$

and S_E^* is determined from equation 13 and equation 5.2 in Table 5.

Implementation of the probabilistic approach requires calculating the spatial and temporal distribution of the first two moments of the statistics, i.e., the average or expected concentration and the variance.

Average concentration equation An equation for the expected value of the concentration is found from the matrix solution of Equation (17), i.e.,

$$\frac{d\langle c \rangle}{dt} = -A \langle c \rangle + \langle S_E \rangle \quad (17)$$

where $\langle \alpha \rangle = E(\alpha)$; the expected value of α .

Variance equation As derived in Di Toro et al., 1985, the variance equation is defined as

$$\begin{aligned} \frac{d\Sigma}{dt} = & -A \Sigma - \Sigma A^T \\ & + \langle | S_E - \langle S_E \rangle || c - \langle c \rangle |^T \rangle \\ & + \langle | c - \langle c \rangle \rangle \langle S_E - \langle S_E \rangle |^T \rangle \end{aligned} \quad (18)$$

where

$$\Sigma = \langle | c - \langle c \rangle || c - \langle c \rangle |^T \rangle \quad (19)$$

and

$$\begin{aligned} & \langle | c - \langle c \rangle || S_E - \langle S_E \rangle |^T \rangle \\ & = \int_0^t e^{-A(t-\tau)} | S_E(\tau) - \langle S_E \rangle || S_E(t) - \langle S_E \rangle |^T d\tau \end{aligned} \quad (20)$$

Specialized input conditions Specifying the time variation of S_E in Equation (20) can be simplified to a certain extent by assuming a simplified behavior for the spectrum of the variance for S_E and then via a superposition principle generating the desired resuspension variance input.

Case 1: White noise

For a flat spectrum or "white noise" with spectral amplitude, Q,

$$\langle |c - \langle c \rangle| | S_E - \langle S_E \rangle |^T = \int_0^t e^{-A(t-\tau)} Q \delta(t-\tau) d\tau = \frac{Q}{2} \quad (21)$$

where δ is the Kronecher delta function.

Case 2: Nonwhite Inputs

If σ is the standard deviation of the entrainment probability distribution and T_{SE} is the entrainment autocorrelation time, then

$$\langle \left\{ \frac{S_E(t+\tau) - \langle S_E \rangle}{\sigma} \right\} \left\{ \frac{S_E(t) - \langle S_E \rangle}{\sigma} \right\} \rangle = e^{-\tau/T_{SE}} \quad (22)$$

and Q for any particular control volume within the reach would become

$$|Q| = 2 |T_{SE}| |\sigma|^2 \quad (23)$$

Log normal distributions of boundary inputs If as is often the case, the probability distributions are lognormally distributed $\langle S_E \rangle$ is found from the lognormal distribution from

$$\mu(S_E) \equiv \langle S_E \rangle = \exp \left[\mu_2(S_E) + \frac{1}{2} \sigma_2^2(S_E) \right] \quad (24)$$

Where: $\mu(S_E)$ is the arithmetic mean of the entrainment in each control volume; $\mu_2(S_E)$ is the log mean of the entrainment in each control volume; and $\sigma_2(S_E)$ is the log standard deviation of the entrainment loading in each control volume. Further statistics include the coefficients of variation in each cv.

$$v^2(S_E) = \exp [\sigma_\lambda^2(S_E)] - 1 \quad (25)$$

and the variance of the entrainment in each cv.

$$\sigma^2(S_E) = - \left| \mu^2(S_E) \right| \left| v^2(S_E) \right|^T \quad (26)$$

METHODOLOGY FOR ESTIMATING ENTRAINMENT CLIMATOLOGY

From equations 17, 18, and 29, it is quite clear that S_E must be known, in particular, the probability distribution for S_E as well as σ , T_{SE} , Q and v . All of the variables are derivable from the probability distribution for S_E , therefore the methodology for determining the entrainment climatology and probability is now developed.

Two procedures for generating the entrainment probability are possible, the first being to directly measure the entrainment for a sufficient number of forcing function combinations to allow full resolution of the forcing function and entrainment probability distributions. The second approach is to synthesize an estimate or prediction of the entrainment using the empirical measures of entrainment and the input data they require. It is only now just possible to measure entrainment and procedures for measuring these data are discussed in a subsequent chapter. For initial estimates, it is possible to synthesize the entrainment climatology using predictions of the bottom shear, bottom condition and the formulae in Table 5. In either case, it is clearly apparent that the driving force in the calculation of the entrainment probability is the continuous variability in the bottom shear which in turn is a function of the wind and flow condition; both of which are stochastic variables. Therefore, it is necessary to first analyze the forcing function climatology which in turn will allow the shear stress climatology to be determined which in turn can be used to determine the entrainment estimate.

Entrainment Estimation Formula

As extracted from Table 5 the entrainment S_E^* is estimated over a time period Δt as a function of the fluid bottom shear stress, τ ; the critical shear stress for erosion, τ_{cr} ; and a function, a , which is in turn inversely proportional to the deposition time, t_d . τ_{cr} and a are dependent on the material characteristics of the bottom, t_d is a function of the time between erosion events, and τ is a function of the local near bottom velocity and oscillatory wave activity. In situ data from the field or forecasted estimates of τ , τ_{cr} , a , and t_d must now be made. This formula (Table 5), while not the most elegant or sophisticated, has the virtue of requiring data that for the most part are either operationally collected over long periods of time or synthesized from deterministic models that have been relatively well verified; particularly, wave forecasting models that will be used to estimate τ . However, the models allowing forecasts of τ and S_E^* have only been sparsely validated with direct field measurements. Therefore, while values for τ and S_E^* , etc., will be synthesized, there remains the goal of organizing a complete field program whose goal is to continue to collect the field data necessary to test these empirical entrainment and shear stress models and verify this procedure.

Bed Characteristics and Critical Shear

Determination of τ_{cr} must come from laboratory data. Such data are available in Parchure and Mehta (1985) and Lee et al. (1981). Table 9 consolidates these results for a variety of different cohesive sediments while Table 9 is the modified Shield's diagram of critical erosion stresses for noncohesive sands and larger silt fractions.

Distributions of sediments specific to the Trenton Channel are discussed in the next chapter.

Bottom Shear Stress

In general the bottom shear stress, as mentioned earlier, arises from currents, waves, or a combination of waves and currents. The interaction between waves and currents is nonlinear. The method to be used here is based upon the original Grant and Madsen (1979) approach as modified for sediment stratification in Glenn and Grant (1987). Simpler approaches such as Sheng (1985) as used by Lee and Bedford (1987) have been used but in general underestimate the actual shear.

As extracted from these articles

$$\overline{\tau}_{cw} = \frac{1}{2} \rho f_{cw} |\overline{U}_b|^2 \alpha \quad (27)$$

in this equation the overbar implies an average over the wave period, T. The wave frequency, ω , wave number, k; and wavelength, L; are defined for a water depth h as follows:

$$\omega = \frac{2\pi}{T}; \quad k = \frac{2\pi}{L}; \quad L = T\sqrt{gh} \quad (28 \text{ a,b,c})$$

The wave average orbital velocity at the bottom is defined as:

$$\overline{U}_b = \frac{H\omega}{2 \sinh(kh)} \quad (29)$$

and the variable α is defined as

$$\alpha = 1 + 2(|\overline{U}_a|/|\overline{U}_b|) \cos \phi_c + (|\overline{U}_a|/|\overline{U}_b|)^2 \quad (29)$$

In equation 29 $|\overline{U}_a|$ is the velocity at the bottom just due to the current and ϕ_c is the angle between the waves and the current.

The future, fcw, factor for combined wave current flow is given by an iterative solution of the following equation

$$\begin{aligned}
 & \left[0.097 \left(\frac{K_b}{A_b} \right)^{1/2} \frac{K}{fcw^{3/4}} \right]^2 + 2 \left[0.097 \left(\frac{K_b}{A_b} \right)^{1/2} \frac{K}{fcw^{3/4}} \right] \left[\frac{V_2}{2 \alpha^{1/4}} \right] \cos \overline{\phi}_c \\
 & = \frac{\alpha^{3/2}}{4} - \frac{V_2^2}{4 \alpha^{1/2}}
 \end{aligned} \tag{30}$$

where

$$V_2^2 = V_{2x}^2 + V_{2y}^2$$

$$V_{3x} = \frac{1}{2\pi} \left[\int_{-\theta_*}^{\pi+\theta_*} (gx^4 + g_x^2 g_y^2)^{1/2} d\theta \right]$$

$$\frac{1}{2\pi} \int_{\pi+\theta_*}^{2\pi+\theta_*} (yx^4 - g_x^2 g_y^2)^{1/2} d\theta$$

$$V_{2y} = \frac{1}{2\pi} \int_0^{2\pi} (gx^2 gy^2 + gy^4)^{1/2} d\theta$$

$$g_x = \frac{|\overline{U}_a|}{|\overline{U}_b|} \cos \phi_c + \sin \theta$$

$$g_y = \frac{|\overline{U}_a|}{|\overline{U}_b|} \sin \phi_c$$

$$\theta_* = \sin^{-1} \left[\left(\frac{|\overline{U}_a|}{|\overline{U}_b|} \right) \cos \phi_c \right]$$

$$\text{for } \left(\frac{|\overline{U}_a|}{|\overline{U}_b|} \right) \cos \phi_c < 1$$

$$\theta_* = \pi/2$$

$$\text{for } \left(\frac{|\overline{U}_a|}{|\overline{U}_b|} \right) \cos \phi_c > 1.$$

When $-\theta_* < \theta < \pi + \theta_*$ shear is positive and negative shear for $\pi + \theta_* < \theta < 2\pi - \theta_*$.

The variable K is defined as

$$K = \frac{1}{2\xi_0^{1/2}} \left\{ \frac{1}{[\text{Ker}^2(2\xi_0^{1/2}) + \text{Kei}^2(2\xi_0^{1/2})]^{1/2}} \right\} \quad (31)$$

where

$$\xi_0 = z_0 / \tau_{cw}$$

$$z_0 = K_b / 30$$

$$\tau_{cw} = \frac{k |\bar{u}_{*cw}|}{w}$$

$$k = 0.4$$

$$A_b = |\bar{u}_b| / \omega$$

$$|\bar{u}_{*cw}| = \left| \frac{1}{2} f_{cw} \right|^{1/2} |\bar{u}_b|$$

The roughness effects are expressed through K_b , i.e.,

$$K_b = K_{bn} + K_{bB} + K_{bT} \quad (32)$$

where $K_{bn} = d$, the Nikuradse roughness based on a d_{50} bed grain diameter.

Also

$$K_{bT} = 3.8 h_{tm}; \text{ roughness due to nearbed transport;}$$

$$h_{tm} = 42 (S+1/2) d \phi_c [(\phi_m^- / \phi_c)^{1/2} - 0.7]^2$$

$$\text{for } \phi_m^- > \phi_c$$

S = specific weight

K_{bB} = $27.7n(n/\lambda)$; roughness due to bedforms; and

$$\phi_m' = \frac{\tau_{bm}'}{\rho(s-1)gd}$$

If $K_b/A_b = d/A_h$ and $fcw = f'cw$, then $\tau_{bm}' = \tau_{cw}'$. Additional formulae include

$$\phi_B'/\psi_c = 18 S_*^{0.6}; S_* = \frac{d}{42} [(s-1)gd]^{1/2}$$

$$\left. \begin{aligned} \eta/A_b &= 0.22 (\phi_m'/\psi_c)^{-0.16} \\ \eta/\lambda &= 0.16 (\phi_m'/\psi_c)^{-0.04} \end{aligned} \right\} \psi_c < \phi_m' < \phi_B$$

$$\left. \begin{aligned} \eta/A_b &= 0.48 S_*^{0.8} (\phi_m'/\psi_c)^{-1.5} \\ \eta/\lambda &= 0.28 S_*^{0.6} (\phi_m'/\psi_c)^{-1.0} \end{aligned} \right\} \phi_m' > \phi_B$$

η = ripple height
 λ = ripple length
 ψ_c = critical shear parameter

and ϕ_B is a break off parameter.

While this is seemingly a very tedious procedure, it is marked by the fact that it requires data that (with the exception of ripple geometry) are relatively easy to obtain. These variables are: the nearbottom current, U_A ; the wave parameters, L , ω and k ; the bed grain size distribution and d_{s0} ; and the ripple geometry. The bed grain size information is obtained as in the previous section. The main variables to be obtained then are the current velocities and the wave information. The following section describes their prediction.

Surface Gravity Wave Field

For purposes of this study, it is assumed that internal waves are not operable at the Trenton River site. No measured data is available to support or deny this assertion and should be a point of future research. Only surface gravity waves are assumed to be present and contribute to the observed fluid sheaer stress at the bottom. In order to provide to equ. 27 the information about the effects of the waves at the bottom, it is necessary to predict the character of the waves at the water surface and then estimate their effect at the bottom.

The information to be determined at surface includes: wavelength, L, wavenumber, k; period, T; frequency, ω ; and wave height, H. It is also necessary to know at each planform location where entrainment is estimated as the average water column depth. The prediction for the surface gravity wave field can be done using common methods available in the Shore Protection Manual (U.S. Army Corps, 1984) or from NOAA-GLERL (Schwab, 1985). Both the methods estimate the above variables given the wind speed, direction, fetch duration and air-water temperature difference. With the exception of fetch and water temperature, these data are operationally collected by the National Weather Service on an hourly basis. Probability distribution are therefore easily calculated.

The spectrum enhanced method in the Shore Protection Manual is used here, therefore a pair of empirical equations are solved for shallow water ($d < 90$ m)

wave parameters H and T:

$$\frac{gH}{U_A^2} = 0.283 \tanh \left[0.530 \left(\frac{gd}{U_A^2} \right)^{3/4} \right] \left| \tanh \left\{ \frac{0.00565 \left(\frac{gF}{U_A^2} \right)^{1/2}}{\tanh \left[0.530 \left(\frac{gd}{U_A^2} \right)^{3/4} \right]} \right\} \right| \quad (33)$$

and

$$\frac{gT}{U_A} = 7.54 \tanh h \left[0.833 \left(\frac{gd}{U_A^2} \right)^{3/8} \tanh \left\{ \frac{0.0379 \left(\frac{gF}{U_A^2} \right)^{1/3}}{\tanh h \left[0.833 \left(\frac{gd}{U_A^2} \right)^{3/8} \right]} \right\} \right] \quad (34)$$

In these equations:

U_A	=	$0.71 U^{1.23}$
U	=	wind speed (m/sec) corrected for air temperature
H	=	wave height
T	=	wave period
F	=	fetch
d	=	water depth

Until such time as it can be shown to be unimportant, it is anticipated that any weather dependent information will have a strong seasonal and monthly variability, particularly due to changes in air-water temperature differences through the season as well as quite different directions in prevailing winds. Therefore, probability distributions will be calculated on a monthly basis.

Velocity and Current Field

A key variable in the shear stress calculation is the near bottom velocity field (U_a) induced by the current field (as opposed to the wave field). The currents are driven, in this case, by gravity as opposed to wind, and will vary from point to point in the flow field, particularly so because of the wide variation in the bottom topography of the channel. The estimate of the velocities must therefore be performed by a model that resolves the planform distribution of the currents and accounts for the variability in the spatial distribution of the currents induced by the variable bottom and shoreline topography.

The model selected here is a relatively standard two-dimensional hydrodynamic model originally developed by Leendertse (1967) and used in modified form by Lee and Bedford (1987) for making calculations in Sandusky Bay. Using a centered staggered-node mesh definition for the vertically averaged U and V horizontal velocities, the following equations are solved by an alternating direction implicit (ADI) scheme.

Continuity

$$\frac{\partial \eta}{\partial t} + \frac{\partial(HU)}{\partial x} + \frac{\partial(HV)}{\partial y} = 0 \quad (34)$$

X-Momentum

$$\frac{\partial HU}{\partial t} + \frac{\partial(HU^2)}{\partial x} + \frac{\partial(HVU)}{\partial y} = -g \frac{\partial \eta}{\partial x} + \frac{\tau_{sx}}{\rho} - \frac{\tau_{bx}}{\rho} \quad (35)$$

Y-Momentum

$$\frac{\partial HV}{\partial t} + \frac{\partial(HUV)}{\partial x} + \frac{\partial(HV^2)}{\partial y} = -g \frac{\partial \eta}{\partial y} + \frac{\tau_{sy}}{\rho} - \frac{\tau_{by}}{\rho} \quad (36)$$

In these equations, η is the water surface elevation above (or below) the still water level; H is the total water column elevation; u and v ; and τ_s and τ_b are the surface and bottom shear stresses expected by the wind and bottom friction, respectively. The wind stress is calculated by the stability dependent method of Schwab (1980) and the bottom shear stress is calculated by the following formulae.

$$\tau_{bx} = \frac{\rho g}{C_c^2} (U^2 + V^2)^{1/2} (U) \quad (37)$$

$$\tau_{by} = \frac{\rho g}{C_c^2} (U^2 + V^2)^{1/2} (V) \quad (38)$$

In equations 37 and 38, the coefficient C_c is the Chezy coefficient which equals $H^{1/6}/N$ and N is the Mannings roughness coefficient. It should be noted

that the above shears represent the retarding effect the bottom exerts on the current field which is not at all the same stress that the sediment "sees" in the resuspension process (equ. 27).

TRENTON CHANNEL SETTING

Introduction

The methodology developed in the previous section is applied in the following section to the Trenton Channel (see Figure 4) as part of the In Place Pollutants activities of the EPA Grosse Ile laboratory. Simultaneous with these estimates a field program, described in a subsequent section, is implemented whose purpose is to begin collecting the data necessary to verify the methodology. The purpose of this section is to review the characteristics of the Trenton Channel that can be determined from existing data.

Data Sources

Operational data for this application has been obtained from the U.S. Army Corps of Engineers - Detroit (USAC-D) and National Oceanic Atmospheric Administration (NOAA) climatology data base in Ashville, North Carolina and the work of Professor J. DePinto at Clarkson College.

From the USAC-D, we have obtained the daily flows in the Trenton Channel as calculated from a model. From NOAA, we have obtained the daily weather information for a period of 13 years from 1971-1983. This period coincides with the time period from daily Trenton Channel flows are available. These data have been obtained for Detroit, Toledo and Cleveland with Detroit serving as the primary data source for this study.

Data extracted from this data base for use in the Trenton Channel study are wind speed and direction for both daily average and daily maximum

conditions and the daily average air temperature. With reference to Figure 4, it is noticed that the only effective directions for wind to generate direct wind waves is along the thalweg (NNE-SSW) although Western Basin wind waves from S, SE and E will propagate indirectly into the south end of the channel.

From Dr. De Pinto, we have extracted a summary of the bottom material characteristics, including grain size distribution, K , at selected sites in the channel.

Brief Summary of Statistical Methods

Certain of the data to be used here are to be statistically analyzed. Methods for such analyses are found in a number of reference works including:

Following is a brief summary of the formulae used here.

1.) Geometric Distribution: The probability $\rho(n)$ that an event A will first occur on the n th Bernoulli trial equals

$$\rho(n) = (1 - \xi)^{n-1} \xi \quad (39)$$

ξ is the probability that an event A in any trial is a constant. The probability that an event A will not occur is $(1-\xi)^n$.

The probability that A occurs at least once is

$$P(n) = 1 - (1-\xi)^n \quad (40)$$

2.) Poisson Distribution The probability, $\rho(n, \tau)$, that n events will occur during time interval τ , equals

$$\rho(n, \tau) = \frac{(\lambda\tau)^n}{n!} e^{-\lambda\tau} \quad (41)$$

for $n = 0, 1, 2, 3, \dots$. The variable X is defined as the average rate of arrival for the process and $\lambda\tau$ is the expected number of events occurring during τ .

3.) Normal and Lognormal Distributions.

The probability $p(x)$ that an independent random variable occurs equals

$$p(x) = \frac{1}{\sigma_x \sqrt{2\pi}} \exp \left(-\frac{(x - \mu_x)^2}{2\sigma_x^2} \right) \quad (42)$$

μ_x is the expected value, $E(X)$, of the distribution, X , of which x is a member and σ_x^2 = variance of X . This distribution is the Gaussian or normal distribution. A logarithmal distribution is defined when a new variable $Z = \log(X)$ is defined.

4.) Type I Extreme Value Distribution

If X is the maximum of n independent random variables ($Y_1, Y_2 \dots Y_n$) then

$$\begin{aligned} F(X < x) &= \text{Prob} (Y_1 < x, Y_2 < x_2 \dots Y_n < x) \\ &= F_{Y_1}(x) F_{Y_2}(x) \dots F_{Y_n}(x) \end{aligned} \quad (43)$$

where the probabilities F_y are called the initial distribution. If the cumulative distribution function for Y converges with increasing y towards unity faster than or equal to an exponential function, then the function is called an exponential type and the Gumbel or Type I extreme value distribution is given by

$$F_{I(X)} = \exp \left\{ -\exp \left[-\frac{(x-\alpha)}{\beta} \right] \right\} \quad \begin{array}{l} -\infty < x < \infty \\ -\infty < \alpha < \infty \\ 0 < \beta < \infty \end{array} \quad (44)$$

In equ 42 α and β are called the location and scale parameter; the mean and standard deviation are defined as:

$$E(x) = \alpha + 0.5772 \beta$$

$$SD(x) = \frac{\pi}{\sqrt{6}} \beta \quad (45)$$

5.) Type II Extreme Value Distribution

If from equation 41

$$\lim_{y \rightarrow \infty} [1 - F(y)] y^k = C \quad (C > 0; k > 0) \quad (46)$$

then the initial distribution is of the Cauchy type and the Type II extreme value distribution is defined as:

$$F_{II}(x) = \exp \left\{ - \left[\frac{(x - \alpha)/\beta}{\gamma} \right]^{-\alpha} \right\} \quad \begin{cases} \alpha < x < \infty \\ -\infty < \alpha < \infty \\ 0 < \beta < \infty \\ \gamma > 0 \end{cases} \quad (47)$$

6.) Risk and Exceedance Probability

If for the type I or II distribution, we define F_I or F_{II} by P , then $\text{Prob}(X > X) = 1 - p$ and the recurrence interval \bar{N} is found from

$$\bar{N} = \frac{1}{1 - p} \quad (48)$$

Alternatively if P is the probability of an event x being equalled or exceeds in the period of record, then

$$p = \frac{1}{\bar{N}}$$

and p is the probability that an event of magnitude x will be equal to or exceed X at least once in any period of record \bar{N} .

Risk is defined as the probability that at least one x will be equal or exceed the value X in any one year or other time or trial interval; i.e.,

$$R = 1 - (1-p)^n \quad (49)$$

where n is the number of years over which the risk is to be determined. For our case, a one year time period is assumed.

Current Climatology

The currents in Trenton Channel have been predicted by the USAC-D (see Figure 4) at Wyandotte and Gibraltar (defining Trenton Channel) by a verified one dimensional flow and elevation model originally developed at NOAA-GLERL by F. Quinn. Thirteen years of daily flows at these two sites have been calculated and we have obtained them from the USAC-D.

The data from USAC-D were analyzed to determine the probability distribution, return period frequency and risk using the standard hydrologic and extreme value analysis methods described above. The data are being analyzed to determine the 13 year probability distribution for all daily flows; the 13 year daily flow probability on a seasonal basis; and the 13 year daily flow probability on a monthly basis. Seasonal and monthly stratification are important because it is anticipated that these will be, for any constant flow value, a very different τ_b from season to season due to the very different wind wave conditions. The seasons defined here do not correspond to the usual definitions; rather they are defined to correspond roughly with periods of dominant weather or thermal conditions. The "ice" season is roughly defined to be from January 1 of any year to mid March and is

therefore marked by very little wind wave activity only currents; the spring heating and flood season is defined from 16 March to 15 June and is marked by high flow and wind events; the summer heating season, 15 June to 30 Sept includes stratification effects and stable air water temperatures, therefore, wind waves are less important; and the storm season from 1 October to 30 December is marked by unstable air sea temperatures which give rise to very aggressive waves but are usually not accompanied by significantly larger river flows.

The 13 years of daily flows were analyzed to determine the suitability of normal, lognormal, Type I and Type II distribution. The data in general did not show dramatically fluctuating values, and flows appeared to be not responsive to most wind/storm events. The exception is, of course, the spring thaw. An extreme value analysis for annual extreme values is in Table 11. Appendices in the final report will contain these data for the monthly and seasonal breakdowns. As can be seen, variation in flows is, in general, quite small which suggests a purely gravity drive flow. Table 12 lists the corresponding risk of exceeding that particular flow in any one year.

Wind Climatology

The hourly values for windspeed, direction and air temperature have been obtained from NOAA for the Detroit station for the same thirteen year period of record sponsored by the USAC-D flow record. Two types of analyses have been performed on these data in order to determine the character of the wind field. The first is a distributional analysis to determine the probability functions for the monthly, seasonal, and annual bases discussed above. Secondly, a zero crossing and conditional probability analysis were performed to better determine the time sequence of wind and storm events.

To simplify the analysis, however, the following assumption has been made. The purpose of the wind field information is to forecast the surface wave fields along the Trenton Channel which in turn are used to assess bottom entrainment shear. Inspection of the Trenton channel sketch in Figure 4 clearly shows that winds blowing across the channel have insufficient fetch to permit any sort of waves to be generated. Therefore, we assume that the only wind information of use to the Trenton Channel is wind blowing down the thalweg, i.e., from N to NE and S to SW. We have, therefore, defined a 30° sector; 15° on either side of the thalweg orientation and only analyze wind from those two directions.

Distributional Analysis-Winds Each hourly wind direction was surveyed to see if it fell in the north or south sector, and each hour this directionality criteria was met, the wind speed, direction, and air temperature stored as a separate data set for analysis. This subset of data was further analyzed to see if it fit any of the previously cited distribution. To determine the seasonal character of the winds, particular attention was paid to this analysis. Tables 13 and 14 contain a summary of the seasonal distributional tests. The Appendix of the final report will contain the annual and monthly results. In general, the Lognormal fit was not acceptable for any season for either south or north winds. The normal distribution was satisfactory for only fall and winter winds from the south and only moderately satisfactory for summer and winter winds from the north. The Log Normal distribution was extremely poor in all aspects and the Type I distribution was uniformly good throughout. Tables 13 and 14 summarize this information.

2.) Distributional Analysis - Temperature Similar analyses were performed in the air temperature data and are summarized in Table 15.

3.) Wind Event Pattern Analysis A conditional sampling approach was used to learn more about the wind events, their duration, and accompanying temperature. The sampling procedure is quite simple. Each hour's data is reviewed and when the wind is from either wind sector, an event is detected and information stored about the duration or number of hours the wind blows from that direction, the average and maximum wind speed from that direction during the event, the average temperature, and the time between events. Interevent results will be discussed in the next subsection. While results showing the conditional probability of an event of a given duration and amplitude will be in the final report, we present here for convenience the summary statistics for each month's events for the eleven year period 1973-1983. Table 16 presents the event summary for North winds and Table 17 presents the event summary for south winds.

4.) Wind Inter-Event Pattern Analysis - Analyses similar to the conditional pattern analysis can be performed for the non-event times particularly for the time between events. Three times were sought; the times between North wind events, the time between south wind events, and the time between all sector events regardless of the North or South direction. Table 18 summarizes these data by month.

Bottom Characteristics

Finally Figure 5 contains the station location map where Dr. J. DePinto and colleagues collected bottom samples. Appendix I contains a summary of the grain sizes found in these data.

FIELD METHODS FOR VERIFICATION

Resuspension Measurement Concept

1.) Hypothesis The concept and method for direct in situ measurement of sediment resuspension was first described in Bedford (et al., 1987b) and in earlier sections of this report). The instrumentation requirements for such a measurement are the ability to sample concentrations densely in both space and time, and velocity measures, both stream-wise and vertical, that are synchronized and closely coupled.

To obtain an entrainment/deposition flux estimate, a control volume is constructed, extending from a height of ξ to a height of η from the bottom, with a square unit cross-section. The heights ξ and η are determined by the instrumentation; η is the location of the two-axis (stream-wise and horizontal) current meter. ξ is as close to the bed as concentration estimates can reliably be made. Typically, the elevation $z = \eta$ should be less than one meter in order to make accurate concentration profile measurements (Bedford, et al., 1987b) and to make velocity measurements within the traditionally expected boundary layer thickness (Grant et al., 1984). The point $z = \xi$, on the other hand, should capture all the suspended load, but not so close to the bottom that concentration estimates cannot be made due to the high concentrations in the bed load. In performing the integration, the average vertical velocity near the bottom is assumed to be vanishingly small, and so any term containing $\bar{w}(z = \xi)$ disappears. Von Leibnitz's theorem is used to account for any variation in the limits of integration, ξ and η (terms 5a and 5b). The full entrainment/deposition equation then becomes

$$\frac{\partial}{\partial t} \int_{\xi}^{\eta} \bar{c} dz + \left\{ D \frac{\partial \bar{c}}{\partial z} + \bar{w} \bar{c} + \overline{w'c'} + \bar{w}_s \bar{c} \right\}_{z=\eta} - \left\{ D \frac{\partial \bar{c}}{\partial z} + \overline{w'c'} + \bar{w}_s \bar{c} \right\}_{z=\xi} \quad (6)$$

$$+ \int_{\xi}^{\eta} \frac{\partial}{\partial x} (\overline{uc}) dz + \bar{c}(z=\xi, t) \frac{\xi z}{\partial t} - \bar{c}(z=\eta, t) \frac{\partial \eta}{\partial t} = 0 \quad (50)$$

Variation in ξ can occur if the rate of erosion or deposition is so high that the bottom moves significantly throughout an averaging period, or if a bedform moves through the control volume. Variation in η (as well as ξ) would be caused by movement of the sampling tower.

Term #4 represents horizontal net sediment flux. Although under conditions of low-frequency, large scale bottom undulations, such flux can become important (McClean and Smith, 1986), it is generally neglected in boundary layers over a flat bottom.

What remains is the turbulent erosion term ($\overline{w'c'}$, term 2 of Equation 50, one part of the resuspension measure we are after, and a cluster of terms that can all be directly measured, or estimated based on sediment characteristics.

The minimum instrumentation, therefore, to make a turbulent resuspension estimate, is a downward-looking acoustic scattering profiling device, sampling the bottom meter of the boundary layer, at one centimeter and one second resolution, and a two-axis (stream-wise and vertical) current meter at a control point within the sampled one meter. Ancillary instrumentation would include a second current meter for two-point stress estimates and a cross-stream current meter to determine if the flow direction may have shifted throughout the course of the experiment. In addition, a pressure gauge would help to measure wave information and calibrate the acoustic concentration measurements, and a thermistor would note temperature variations.

The interfacing of field data with model predictions, therefore, may be divided into three tasks: 1) screening and converting raw data into properly

scaled, rotated and averaged velocities, and calibrated concentrations; 2) determining if the conditions of the field experiment satisfy the assumptions of both the resuspension equation and stress estimates, and 3) if assumptions are not fully satisfied, applying appropriate correction procedures to the data.

2.) Converting Raw Data to Velocity Ideally, the horizontal and vertical velocity probes are exactly aligned with the stream-wise horizontal and vertical coordinates. Emplacement of the tower, however, is a difficult and inexact process. It may land on an uneven bed or incorrect orientation. But once in place, it generally cannot be moved. It falls then to post-collection analysis to correct for tilt encountered in the field. The necessity for correction is pointed out by Heathershaw and Simpson (1978). Errors in turbulent stress estimates arise from errors in the covariance of u and w . The latter can vary by 10% per degree of tilt. Aggravating the situation is the fact that the zero point of the current meter, the reading that the current meter gives when the true velocity is zero tends to drift.

One method of obtaining the instrument tilt and zero point simultaneously is to perform a linear regression of the vertical probe reading against the horizontal reading. If we assume a constant tilt and zero point, then the relation between the true stream-wise coordinate velocities (U, W) and the readings (u, w) is

$$U = (u - d) \cos \theta + (w - d) \sin \theta \quad (51)$$

$$W = - (u - d) \sin \theta + (w - d) \cos \theta \quad (52)$$

where d is the zero point and θ is the angle through which the readings must be rotated to obtain stream-wise coordinates. Alternatively, we could write

$$(u - d) = U \cos \theta - W \sin \theta$$

$$(w - d) = U \sin \theta + W \cos \theta.$$

Eliminating U and solving for w in terms of u, d, θ , and w gives,

$$w = u \tan \theta + d(1 - \tan \theta) - W/\cos \theta. \quad (53)$$

The above equation has the form of a linear relation with added noise, where $\tan \theta$ is the slope and $d(1 - \tan \theta)$ is the intercept. The term $W/\cos \theta$ is the residual, since by assuming stream-wise coordinates, the long-term average of W must be zero. The standard form for a linear regression (Bendat and Piersol 1971) with slope a and intercept b

$$w_i = au + b$$

is given by

$$b = \bar{w} - a\bar{u}$$

and

$$a = \frac{\Sigma(u - \bar{u})(w - \bar{w})}{\Sigma(u - \bar{u})^2}$$

Substituting the above expression for w

$$\begin{aligned} a &= \frac{\Sigma(u - \bar{u})(u \tan \theta - u \bar{u} \tan \theta)}{\Sigma(u - \bar{u})^2} + \frac{\Sigma(u - \bar{u})(w - \bar{w})/\cos \theta}{\Sigma(u - \bar{u})^2} \\ &= \tan \theta + \frac{\Sigma[(U - \bar{U})(W - \bar{W})]}{\Sigma(u - \bar{u})^2} - \frac{\Sigma(W - \bar{W})^2}{\Sigma(u - \bar{u})^2} \tan \theta \end{aligned}$$

The first expression on the right-hand side is the result were W identically zero. The second expression is roughly the UW correlation, which should go to zero over long time. The third expression is the variance in W divided by the variance in u. Because W is not known before untilting is done, the procedure would have to be iterative if W is not much less than u.

Another method of untilting involves plotting a histogram of the velocity energy $((u-d)^2 + (w-d)^2)$ in each of 360° increments. The peaks of the histogram would be diametrically opposed and lie along the tilting plane. Any error in d would show up as an angle between the two peaks not equal to 180°.

3.) Converting Backscatter Signal to Concentration Estimates

The received acoustic backscatter intensity, from a field of particles located at distance z from the transducer, at time t, is given by a single scattering theory as

$$I(z,t) = N + f(z, T, p) \int_0^z n(z, t) \exp(\alpha \int_0^z n(s, t) ds) \quad (54)$$

where N is the intensity of additive (as opposed to unbiased) noise, f is the response function, a function of the instrument and ambient temperature and pressure, n is the number of scatterers in the sampling volume, h is a function of the scattering characteristics of the sediment, and α is a coefficient for attenuation due to scatterers. Under the assumption that the characteristics of the scattering population (including size distribution, but excluding total concentration) are effectively invariant in time and space, the concentration is strictly proportional to n. The product, n h, may then be replaced by c h', and the equation is solved for c to produce

$$c(z, t) = (I(z, t) - N) / (h' f(z, T, p) \exp(\alpha' \int_0^z c(s, t) ds)). \quad (55)$$

The goal is that f, the response function, be determined to within a constant factor, by acoustic modeling and, if necessary, instrument calibration with N and h' as site-specific constants. The value of h' is determined by comparing the concentration in a grab sample taken at a known height with the received signal at that height and approximate time. Further discussion appears in Libicki et al., 1987a, b., but an additional comment on noise is necessary.

Term 2 of Equation 50, $w'c'$, the turbulent flux at the top of the control volume is estimated from the instantaneous values of the velocity and the concentration at the level of the current meter. The estimate is biased downward by the limited sampling frequency (one sample per second). It is biased upward by extraneous contributions from instrument noise, Poisson statistics and configurational noise.

To combat such noise, the CDART system employs signal conditioning and integration and rapid ensemble averaging. Theoretical calculations indicate that these measures enable a signal to noise ratio of 9.6, given a sufficiently large flow through the isonified volume.

Rapid ensemble averaging involves taking a profile 32 times per second and averaging it in real time to form one retained average profile each second. Although the sampling frequency is once per second, true temporal resolution can be much less than that if further averaging is required to produce reliable data. An indication of the relative sizes of turbulent variation and noise can be provided by spectra of the concentration time series. Power spectrum density estimation for the data is based upon the Periodogram Method (Rabiner, et al., 1979), which, in turn, employs the Fast Fourier Transform. Each block is divided into 13 overlapping segments, each with 512 points. Each segment is detrended by subtraction of a linear regression of the data. Spectral leakage is minimized by data tapering with a Hamming window. Finally, confidence intervals are assigned by the chi-squared relation (Otnes and Enochson, 1978). Spectra are plotted in the traditional wave-number space, with the wave number being calculated from the average velocity from each block.

The 3 MHz transducer has a 3-dB beam width of 1.5 cm at 1 meter, and so at flow rates above 1.5cm/sec, all sources of noise -- thermal, configura-

tional, and Poisson, ought to be uncorrelated from one sample to the next, and exhibit a flat spectrum (Otnes and Enochson, 1978). By contrast, any species carried by a turbulent flow field has a spectrum that decays as a power of the wave number (which power is a function of the flow regime and mechanisms governing the production and destruction of the species). Based on the foregoing assumptions, a turbulent spectrum with noise would plot with an initial slope that flattens out at high wave numbers. Further, the point at which the slope flattens is that point at which noise begins to predominate over turbulent variation. It marks, for a particular instrument under a particular set of field conditions, the true temporal resolution of the instrument. For the second block of the above data set, this works out to approximately three seconds (twice the sampling frequency, or two seconds, is the upper limit possible, due to Nyquist constraints). By assigning the flat portion of the spectrum to noise, it is possible to extrapolate that value back through all the frequencies and estimate the total noise in the data. For the eight blocks of the deployment, the average signal to noise ratio is 7.8, with a range from 4.2 to 10.3 (recall that the theoretical signal to noise ratio for the 3 MHz system was 9.6).

Instrumentation - Trenton Channel

Introduction To sample several sites in and around the Trenton Channel over short periods of scheduled boat time, a rapid deployment scheme was used. The OSU CDART (Coastal Data Acquisition and Retrieval Tower) system was designed to be used in deeper water (15 ft.-100 ft.), but had performed satisfactorily in two surface-connected deployments from the RV Blue Water in October 1984 and July 1985. These investigations were done in 10-12 ft. of murky water along a bulkhead in the Monroe Harbor turning basin. With the Bluewater

secured in position, it was possible to place a small PVC frame holding the instrument above the bottom astern of the Blue Water, with the probe cables running up over the gunwale and into the lab amidships. There, they were connected to the data collection computer.

If the Blue Water had sufficient depth to maneuver and subsequently anchor securely in place, it seemed feasible that the same general set up could be used in selected sites in the Trenton Channel. Instead of the bulky PVC frame used previously, a minimum cross-sectional area tower was configured and used. To guarantee proper positioning with respect to the bottom, mean currents and/or wave directions the tower was positioned and secured by diver. This did not seem to present a problem, since diver-obtained sediment cores were needed from the sites during the tower deployments. Care was taken not to expose the diver to corrosive, toxic or carcinogenic substances, and a scheduled set of preliminary chemical and biological investigations of all sites would be used to rule out hazardous areas before the tower was deployed.

Other than these considerations the operating aspects of the OSU system remained essentially as in the Raisin River study. On the new tower, the instruments were positioned to meet the instrument spatial resolution requirements discussed in the previous section. Existing computer software provided sufficient sample density and speed to study conditions existing at the sites. Although having the microcomputer assembly open in the vessel/lab exposed the circuitry to dust, fumes, smoke, humidity and vibration, no major problems resulted. With 75 ft. of instrument cable to work with, sites of up to 25 - 30 ft of depth were probed, provided the Bluewater was able to double or triple anchor securely and safely in place.

Instrumentation Components The instrumentation configuration used in the study employs the 3 MHz Edo Western profilometer as the main probe. Looking downward toward the bottom sedimentation angle slightly less than vertical, it sends a 10 μ s pulse of 3 MHz sound through the water column. It then immediately receives the various echoes returning from the reflecting suspended particles and bottom, while simultaneously sending a voltage corresponding to the path reflectivities to the data collection circuitry. There the signal is digitized into 110 readings from bins along the beam path. These profiles are taken 32 times per second and are ensemble-averaged on board to produce a 1-second averaged profile for storage to tape.

Two Marsin McBirney 511 (small ball) dual-axis electromagnetic current meters are mounted directly downstream of the profile beam to prevent eddies formed downstream of the probes, from interfering with the profile, yet allowing the closest possible spatial correlation between the two sets of measurements. The lower current meter, mounted 25 cm above the bottom measures the downstream horizontal component (x) and the vertical component (z) of the water velocity at that height. The upper current meter, mounted at 1.1 m above the bottom, measures the downstream horizontal component (x) as well as the cross-stream horizontal component (y) of velocity at that height. Analog signals are converted to digital information.

A Sea Tech (5 cm) optical turbidimeter is aligned with its port at mid-profile, yet out of the way of the beam, to monitor water clarity during profiling. A pressure transducer mounted above the other probes is used to record variations in water surface level above the study site, and a thermistor probe monitors water temperature during sampling. All are connected separately to the data collection computer and their analog signals are converted on board to digital information for storage.

All sampling routines written for the CDART system are based on a 1 Hz unit frequency. All measurements are taken once a second, with the exception of the current meters and pressure gauge, which are all sampled twice during that period. In all "rapid deployments", continuous sampling at the 1 Hz rate assures maximum data density over the available observation time, with the instruments and data collection circuitry running constantly until being reset at the end of sampling. While running the sampling, it is possible to use an oscilloscope and voltmeter to observe incoming signals for any irregularities that may signal equipment malfunction or undesirable movement of the tower. As all data are being collected they are fed directly onto a 60 megabyte Sea Data streaming tape drive.

Trenton Channel Deployment Summary

Table 19 contains a summary of the deployments to date.

Data Analysis

At the time of this writing, data analysis is just proceeding and will continue so for the next year.

REFERENCES

- Bedford, K. and M. Abdelrhman, 1987, "Analytical and Experimental Studies of the Benthic Boundary Layer and their Applicability to Near-Bottom Transport in Lake Erie," in: Lake Erie Synthesis Volume, Journal of Great Lakes Research. To appear.
- Bedford, K., C. Libicki, O. Wai, M. Abdelrhman, and R. Van Evra, 1987a, "The Structure of a Sediment Boundary Layer in Central Long Island Sound," in: Proc. Physics of Estuaries and Shallow Bays, to appear, Springer Verlag Pub. Co.
- Bedford, K., O. Wai, C. Libicki and R. Van Evra 1987b "Sediment Entrainment and Deposition Measurements in Long Island Sound," J. Hydraulic Engineering ASCE 113(10), pg.
- Bowden, K. F., 1973, "Physical Problems of the Benthic Boundary Layer," Geophysical Surveys, Vol. 3, pg. 255-296.
- Boyce, F. M., 1974, "Some Aspects of Great Lakes Physics of Importance to Biological and Chemical Processes," J. Fisheries, Res. Board of Canada, 31 (5), pg. 689-730.
- Caldwell, D. R. and T. Chriss, 1979, "The Viscous Sublayer at the Sea Floor." Science, 205, pg. 1131-1132.
- DiToro, D., et al., 1985, Ch. 3 in EPA Final Rept. on Raisin River/Monroe Harbor Cooperative Agreement.
- Fisher, F. and V. Simmons, 1977, "Sound Adsorption in Sea Water," J. Acoustical Soc. Amer., 62(3), pg. 558-564.
- Fredsoe, J., 1984, "Turbulent Boundary Layer in Wave-Current Motion," J. Hyd. Engrg., ASCE, 110(8), pg. 1103-1121.

- Glenn, S. and W. Grant, 1987, "A Suspended Sediment Stratification Correction for Combined Wave and Current Flows," J. Geophys. Res., 92(C8), pg. 8244-8264.
- Grant, W. D. and O. S. Madsen, 1979, "Combined Wave and Current Interaction With a Rough Bottom," J. Geophys. Res., 84(C4), pg. 1797-1808.
- Grant, W., A. J. Williams and S. M. Glenn, 1984, "Bottom Stress Estimates and Their Prediction on the Northern California Continental Shelf During CODE-1: The Importance of Wave-Current Interaction," J. Phys. Oceanography, 14, pg. 506-527.
- Hayter, F. J., and A. J. Mehta, 1982, Modeling of Estuarial Fine Sediment Transport for Tracking Pollutant Movement. Technical Report UFL/COEL - 82/009, U.S. Environmental Protection Agency, December.
- Heathershaw, A. D., 1979, "Turbulent Structure of the Bottom Boundary Layer in a Tidal Current," Geophysical Journal of the Royal Astronomical Society, 58(2), pg. 395-430.
- Heathershaw, A. D. and J. H. Simpson, 1978, "The Sampling Variability of the Reynolds Stress and its Relation to Boundary Shear Stress and Drag Coefficient Measurements," Estuarine and Coastal Marine Science, 6, pg. 263-274.
- Jonsson, I. G., 1963, "Measurements in the Turbulent Wave Boundary Layer," Proc. 10th IAHR Conf., London, pg. 85-92.
- Krone, R. B., 1972, A Cohesive Sediment Transport Model. Technical Bulletin 19, U.S. Army Corps of Engineers, June.
- Lee, D. and K. Bedford, 1987, "Resuspension and Sorting Effects on Tributary Sediment Loads to Lake Erie," Proc. 22nd IAHR Conf., Lausanne, Switzerland, Aug 30 - Sept 4.

- Lee, D. Y., S. W. Kang and W. Lick, 1981, "Deposition and Transport of Fine-Grained Sediments," J. Great Lakes Res. 7, pg 224-233.
- Lumley, J. L., 1978, "Two-Phase and Non Newtonian Flows," Topics in Applied Physics, ed. by P. Bradshaw, Springer Verlag, New York, pg. 289-324.
- McCave, I.N., (Editor), 1976, The Benthic Boundary Layer. Plenum Press, New York.
- McClellan, S. and J. Smith, 1986. "A Model for Flow over Two-Dimensional Bedform," J. Hydraulic Engineering, ASCE 112(4), pg. 300-317.
- Nihoul, A. and C. Hollister, 1986, Deep Ocean Sediment Transport, Elsevier Pub. Co.
- Otnes, R. and L. Enochson, 1978, Applied Time Series Analysis. Vol. I, John Wiley and Sons.
- Panchure, T.M., and A. J. Mehta, 1985. "Erosion of Soft Cohesive Sediment Deposits," J. of Hydraulic Engineering, 111(18), pg. 1308-1326.
- Parteniades, E., 1962, A Study of Erosion and Deposition of Cohesive Soils in Salt Water. Ph.D. thesis, University of California, Berkeley.
- Parthenaides, E., 1971, Chapter 25, Erosion and Deposition. In: H. W. Shen (Ed.), River Mechanics, Vol. II, Colorado State University.
- Pierce, A.D., 1981, Acoustics: An Introduction to Its Physical Principles and Applications, McGraw Hill Pub. Co.
- Rabiner, L., R. Schafer and D. Dlugos, 1979, "Periodogram Method for Power Spectrum Estimation," in: Program for Digital Signal Processing, ed., IEEE Digital Signal Processing Committee, IEEE Press.
- Scarlato, P. D., 1981, "On the Numerical Modeling of Cohesive Sediment Transport," J. of Hydraulic Research, 19(1), pg. 61-67.
- Schwab, D. J., 1980, "Simulation and Forecasting of Lake Erie Storm Surges," Mon ... Weather Review, 106, pg 453-460.

- Schwab, D., J. Bennett and A. Jessup, 1984, "A Two-Dimensional Lake Wave Prediction System," NOAA Tech Memo ERL-GLERL-38, Ann Arbor, MI.
- Sheng, P. and W. Lick, 1979, "The Transport and Resuspension of Sediments in a Shallow Lake," J. of Geophysical Research, 84(c4), 1809-1826.
- Sternberg, R. W., 1972, "Predicting Initial Motion and Bedload Transport of Sediment Particles in the Shallow Marine Environment," in: Shelf Sediment Transport: Process and Pattern, Ed: Swift, D., Duane, J. P., and Pilkey, O. H., Dowden, Hutchinson, and Ross, Stroudsburg, PA., pg. 61-82.
- Teleki, P. G., 1972, "Wave Boundary Layers and Their Relation to Sediment Transport," 1972, in: Shelf Sediment Transport: Process and Pattern, Eds.: Swift, D.J.P., Duane, J.B. and Pilkey, O.H. Dowden, Hutchinson, Ross, Stroudsburg, PA., pg. 21-59
- Uchian, C. G. and W. J. Weber, Jr., 1980, "Modeling of Transport Processes for Suspended Solids and Associated Pollutants," in: Fate and Transport Case Studies, Modeling, Toxicity, Ann Arbor Science Publishers.
- Vanoni, V. A., editor, 1975, Sedimentation Engineering. American Society of Civil Engineers.
- Yalin, M., 1978, Mechanics of Sediiment Transport, Pergamon Press, NY.
- Ziegler, C. and W. Lick, 1986, "A Numerical Model of Resuspension, Deposition and Transport of Fine-Grain Sediments in Shallow Water," Rept. Dept. Mech. Engrg. U. Cal. Santa Barbara, USSB-ME-86-3.

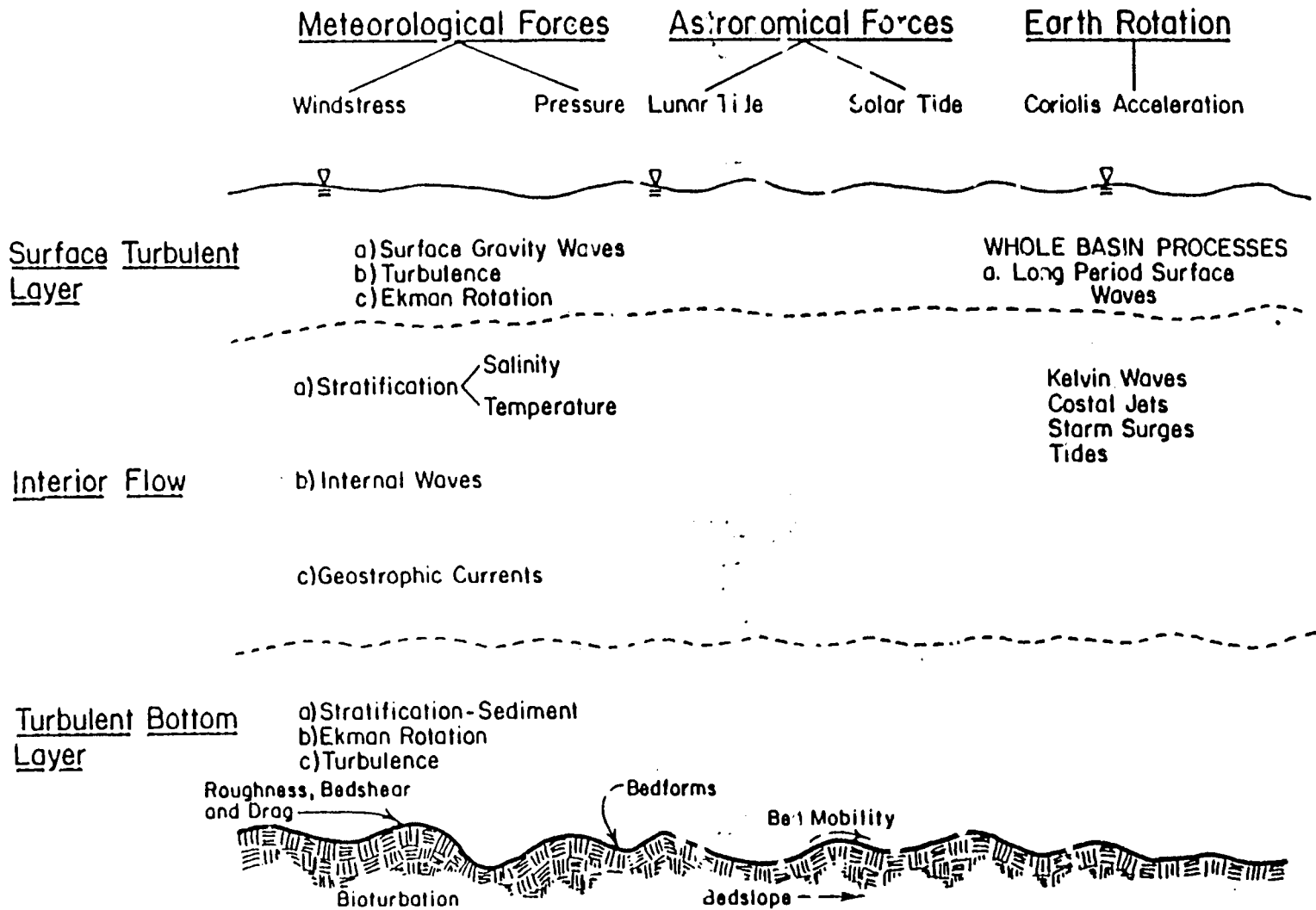


Figure 1 Schematic of Factors Affecting Entrainment and Resuspension

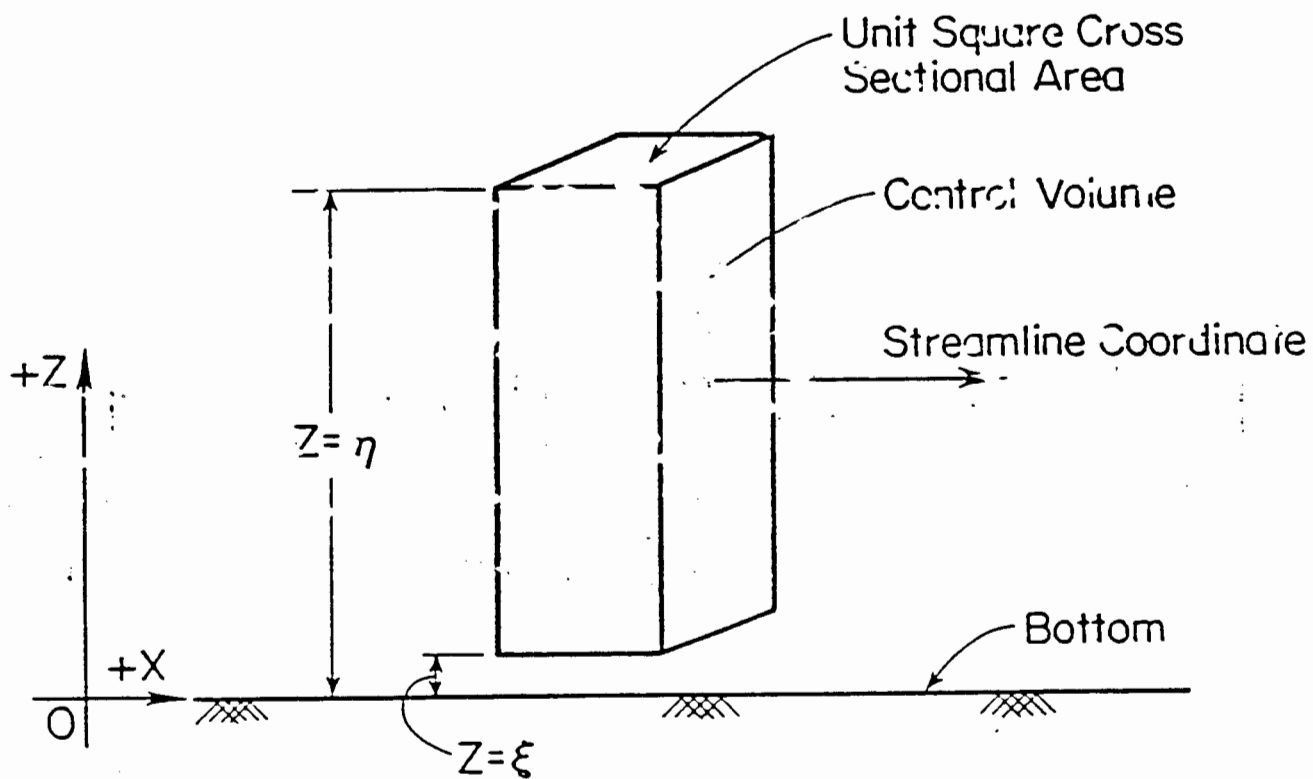


Figure 2 Coordinate System Definition

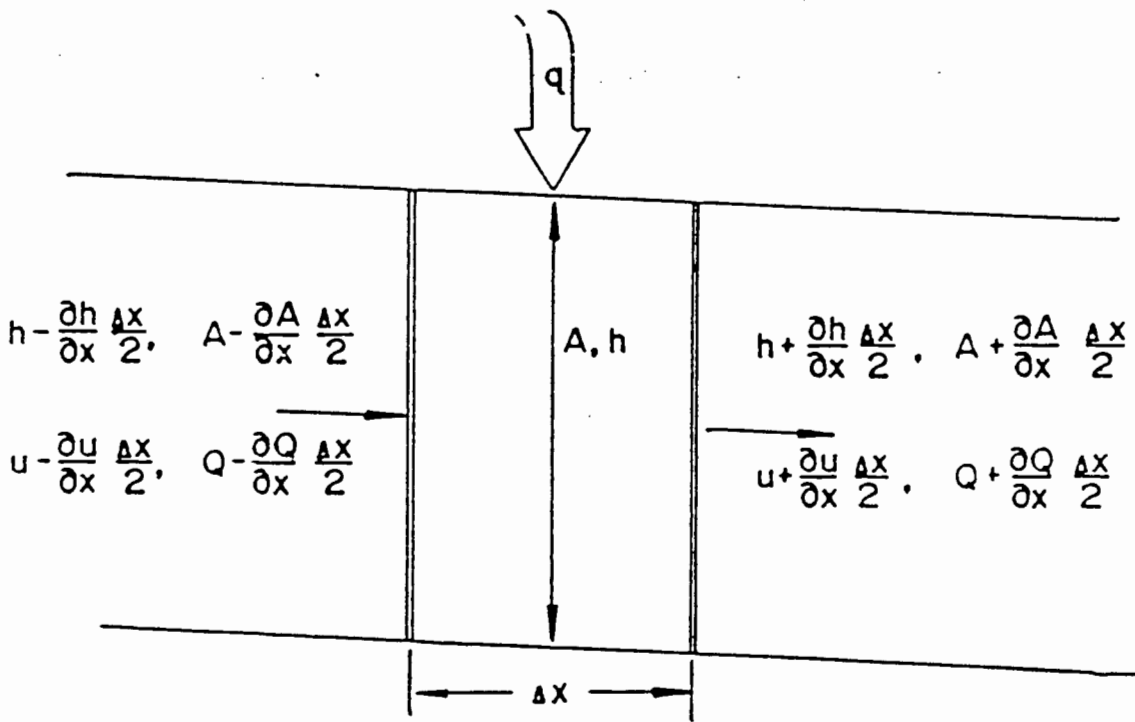
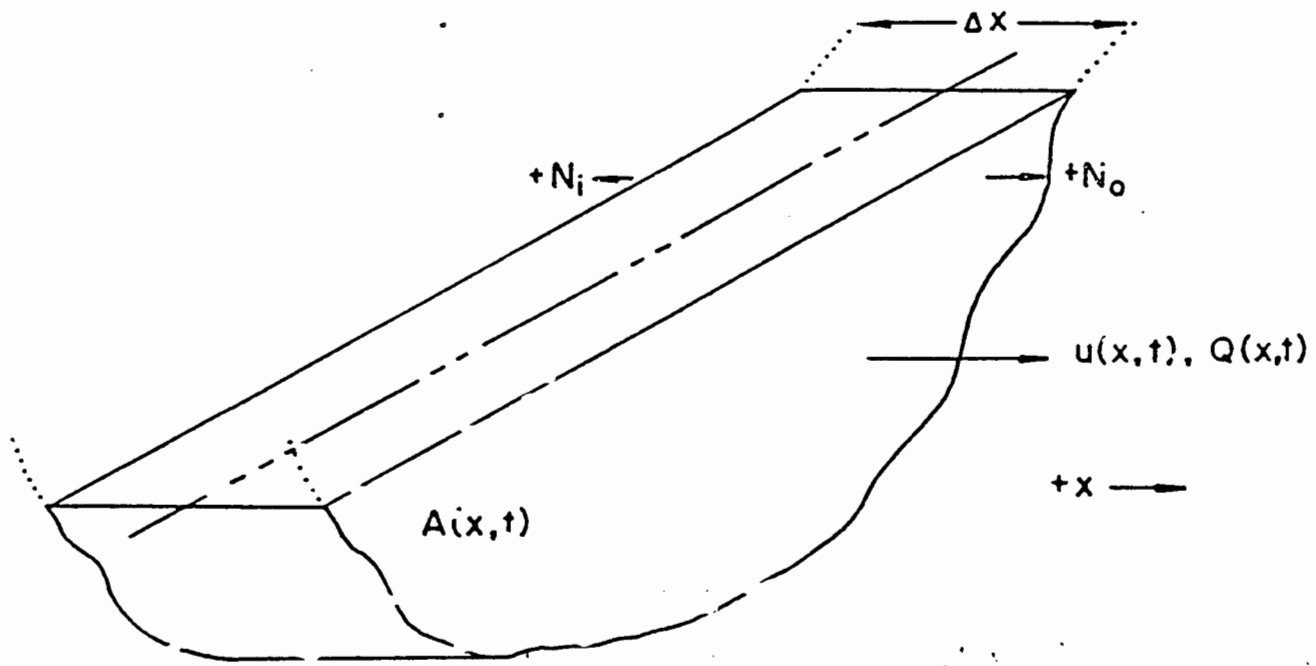


Figure 3 Control Volume Definitions-River Model

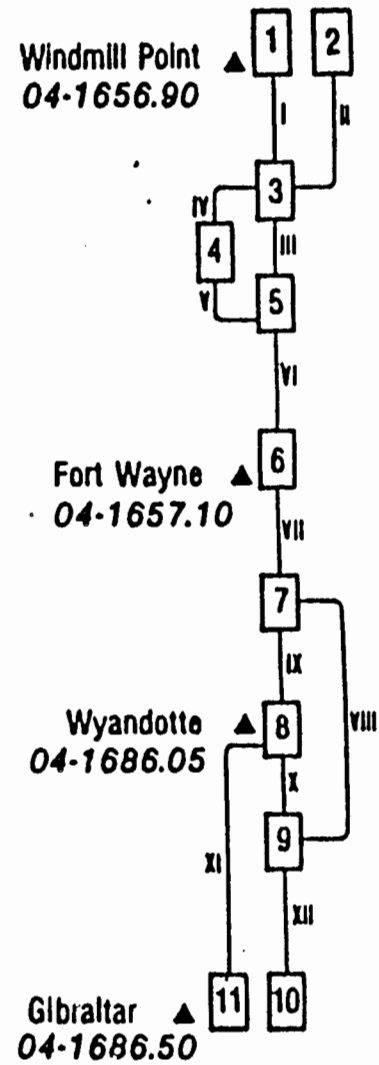
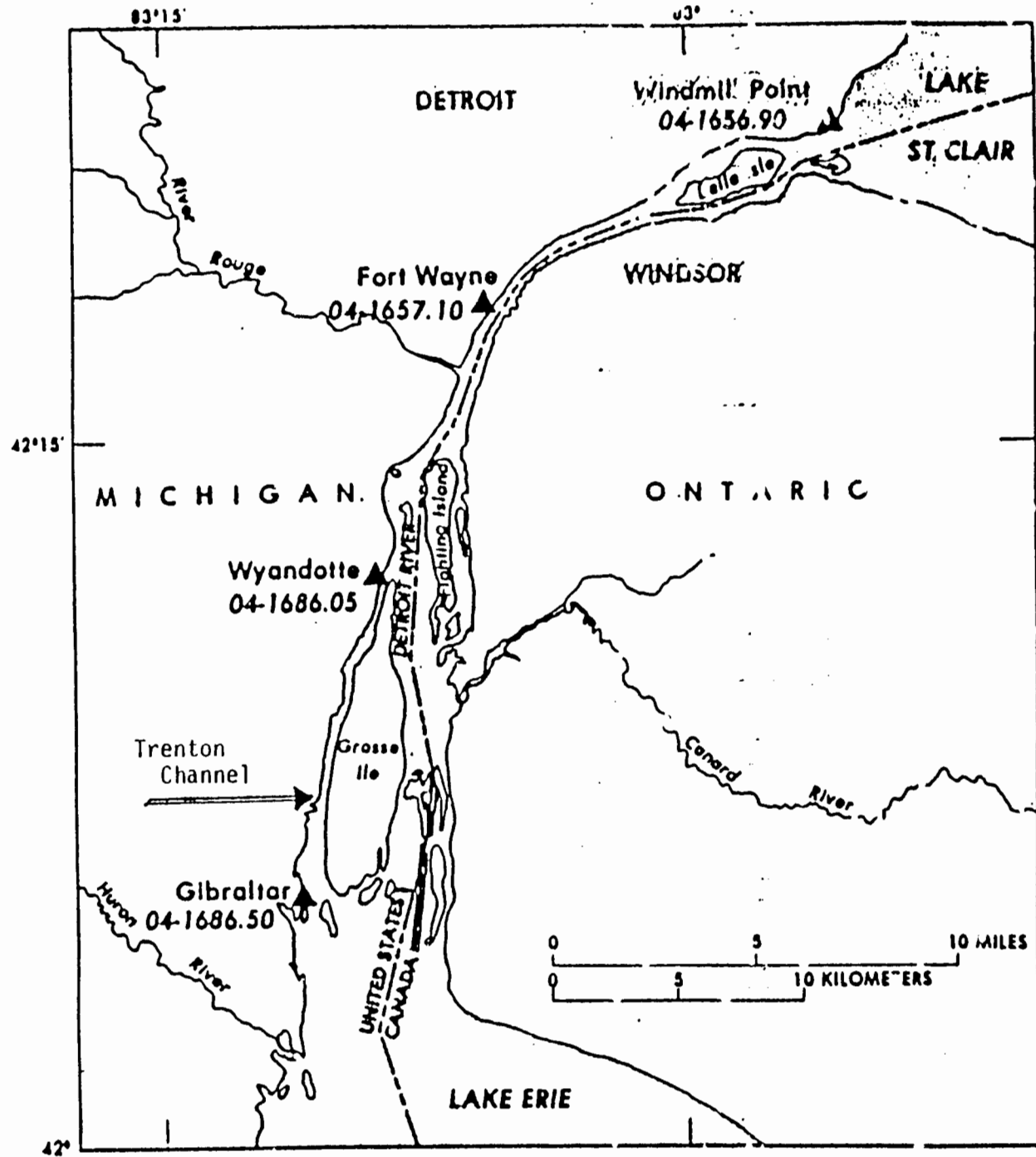


Figure 4 Trenton Channel/Detroit River Map

Table 1

(After Boyce 1974) A partial list of motions and their associated time and space scales. Letters in parentheses refer to the nature of the scale used. M, amplitude of motion; S, distance over which phenomenon varies significantly; P, period; T, time interval over which phenomenon varies significantly; C, wave speed; V, vertical particle velocity; H, horizontal particle velocity. The governing terms in the equations of motion and continuity are listed in column 6 according to the code: 1, time-dependent horizontal accelerations; 2, time-dependent vertical accelerations; 3, advective component of horizontal acceleration; 4, advective component of vertical acceleration; 5, Coriolis force; 6, pressure gradient force due to slope of free surface; 7, pressure gradient force due to slope of the thermocline; 8, pressure gradient force due to atmospheric pressure field; 9, variations in bottom topography; 10, wind energy/stress; 11, internal stresses arising from horizontal current shear; 12, internal stresses arising from vertical current shear; 13, friction against boundaries; 14, potential energy changes due to surface heating and cooling; 15, astronomical tidal-generating forces due to sun-earth-moon gravitational potential fields; 16, potential energy changes due to temperature and salinity changes.

(1) Phenomenon	(2) Length Scale		(4) Time scale	(5) Velocity scale	(6) Dynamic major components
	Horiz.	Vert.			
a. Wind driven surface gravitational waves	10 m(S)	1 m(M)	15(P)	10 m/s(C) 1 m/s(V,H)	1,2,6,10
b. Surface gravitational waves - seiches	100 km(S)	10 cm(M)	2-10 d(P)	2 cm/s(H)	1,6,10
c. Short freely propagating internal waves	100 m(S)	2 m(M)	5 min(P)	2 cm/s(V)	11,2,7,10
d. Long propagating internal waves steered by topography	10 km(S)	2 m(M)	1 day(T)	50 cm/s(C)	1,5,7,9,10
e. Internal gravitational standing waves or seiches	10 km(S)	2 m(M)	16 d(P)	10 cm/s(H)	1,5,7,10
f. Surface wind drift	-	10 cm(S)	-	2 cm/s(H)	10,12
g. Coastal currents	10 km(S)	-	1 day(T)	10 cm/s(H)	all
h. Upwelling and downwelling	10 km(S)	10 m(M)	1 day(T)	1 cm/s(V)	all
i. Wind driven horizontal circulation	100 km(S)	100 m(S)	1 day(T)	10 cm/s(H)	all
j. Geostrophic current	-	-	1 day(T)	3 cm/s(H)	5,6
k. Langmuir circulations vertical mixing of epilimnion	-	10 m(S)	1 h(T)	1 cm/s(V)	1,2,3,4,10,12,14, and others
l. Formation and decay	-	10-100 m(S)	1 mo(T)	-	10,12,14
m. Tidal waves:					
a) diurnal (M ₂ , S ₂ , M ₂)	Earth radius	-	1 day(T)	-	1,2,5,15
b) semidiurnal (M ₂ , S ₂ , M ₂)	-	-	1/2 day(T)	-	1,2,5,15

Table 2 Summary of the Erosion Source Terms

Erosion Source Term	Equation Number
E. Parthiendaides:(1962) $S_e = E \left(\frac{\tau_b}{\tau_{ce}} - 1 \right)$	2.1
F. Parthiendaides. (1971) $S_e = \frac{A D_b \gamma_s}{t(\tau_c)} \left[1 - \frac{1}{\sqrt{2\pi}} \int_{-a}^a \exp -\left(\frac{w^2}{2} \right) dw \right]$	2.2
P. D. Scarlatos: (1981) $S_e = C_s B \exp(-Bt)$	2.3
Hayter and Mehta: (1985) $S_e = \epsilon_0 \exp \alpha \left(\frac{\tau_b}{\tau_{ce}} - 1 \right)$	2.4
Parchure and Mehta: (1986) $S_e = \epsilon_f \exp[\alpha(\tau_b - \tau_s)^{1/2}]$	2.5
W. Lick:(1986) $E_{net} = \frac{a_0}{t_d^2} \left(\frac{\tau_b - \tau_{ce}}{\tau_{ce}} \right)^2$	2.5

Table 3 Summary of the Deposition Sink Terms

<u>Deposition Sink Term</u>	<u>Equation Number</u>
R. B. Krone: (1986) $S_d = \frac{-PV_s C}{h}$	3.1
Y. P. Sheng: (1983) $S_d = V_s C$	3.2
W. Link: (1986) $S_d = B_r C$	3.3
Uchrin and Weber: (1980) $D \frac{\delta C}{\delta z} = -\phi V_s C$ where $\phi = \frac{\alpha D_p}{(B + D_p)} (U_* - U_{*cr})$	3.4
Hayter and Mehta: $\left(\frac{\Delta C}{\Delta t}\right)_d = \frac{-0.434}{2\sqrt{2\pi}\sigma_2} \exp\left(\frac{(-t_c^2/2)}{t} C_o\right)$ $\left[1 - \operatorname{erf}\left(\frac{1}{2\pi} \log_{10} \left[\frac{(\tau_b^* - 1)}{4 \exp(-1.27\tau_{bmin})} \right]^{2.04} \right) \right]$	3.5 (1985) *

Table 4 Summary of the Equations for Settling Velocity

Settling Velocity Equation	Equation Number
Stoke's Law: Vanoni(1975)	4.1
$V_s = \frac{2r^2(\rho_s - \rho_w)g}{9\nu}$	
P.B. Krone: (1972)	4.2
$V_s = K_s C^{4/3}$	
N. Hawley: (1983)	4.3
$V_s = ad_p^b$	

Table 5

The Lick Entrainment and Deposition Model (after Ziegler and Lick, 1986)

FORMULA	EQUATION NO.
$S_D^* = w_s c \quad d > 0.5 \mu m$	5.1
$S_E^* = \frac{d\tau}{dt} \rightarrow \quad \epsilon = \int_0^{\Delta t} S_E^* dt$	5.2
$\epsilon = a \left\{ \frac{\tau - \tau_{cr}}{\tau_{cr}} \right\}^m \quad \tau > \tau_{cr}$	5.3
$\epsilon = 0 \quad \tau < \tau_{cr}$	5.4

where:

- a = a_0/t_d^n
- t_d = time after deposition (days)
- τ = local fluid shear (dynes/cm²)
- τ_{cr} = critical shear stress for erosion
(~ 1.0 dynes/cm²)
- a_0 = coefficient ($\cong 8 \times 10^{-3}$, but is sediment dependent)
- n } exponents = 2.0
- m }
- w_s = settling velocity for a particular grain size
- c = concentration of sediment in that grain size

Table 6

Methods for Calculating Bottom Stress from Constant Stress Data

Formula Name	Relevant References	Formulae	Definitions	Comments
1.) Empirical Approach	Sternberg (1968,1972)	$\tau_b = C_{D100} \rho \bar{u}_{100}^2$	ρ = density C_{D100} = drag coefficient estimated at 100cm off bottom \bar{u}_{100} = time avg velocity 100cm above bottom	An often used engineering approach; Assumes validity of log region 100cm thick which is not often true; Very large error in τ_b estimates.
2.) Two Point Method	Caldwell and Chriss, (1979)	$\tau_b = \rho u_*^2 = \rho \frac{k(\bar{u}_{z1} - \bar{u}_{z2})^2}{\ln z_1 - \ln z_2}$	u_* = friction velocity z_1, z_2 = velocity measurement at points	Holds for smooth and rough flows; Heights z_1 and z_2 are usually separated by one decade; The time average required for the u_* velocity is one decade longer than the u_{z1} flow velocity.
3.) Direct Reynolds Stress	Heathershaw (1978)	$\tau(z) = -\rho(\overline{u'w'})$	$\overline{u'w'}$ = correlation (temporal) of horizontal and vertical velocity fluctuations u' and w'	Can't estimate the bottom stress; therefore not usable for estimating resuspension. Very susceptible to noise from wave activity.
4.) Inertial Dissipation Method	Deacon (1959)	$\tau_b = \rho(c\epsilon z)^{2/3}$ and $c = \frac{\phi(k^*)}{\alpha_3} k^{*5/3}$	z = distance above bottom c = dissipation (k^*) $\phi(k^*)$ = wave-number (k^*) spectrum (Eq.9) in inertial subrange. $\phi(k^*) = \alpha_3 \epsilon^{2/3} k^{*-5/3}$	Implies production and dissipation of energy are in equilibrium and wave activity is outside the range inertial subrange. Depends on small range of wavenumbers and validity of Frozen turbulence hypothesis
5.) Log Profile Method	Grant et. al. (1984)	Data/Regression Fit To $\log z = \frac{k}{2.3u_*} \bar{u} + \log z_0$	z_0 is roughness length.	Slope of data-fit line to equation gives u_* while intercept gives z_0 . Regression coefficients of 0.997 (Grant et. al. 1984) or greater ensure the steady nonwave affected flow required for this technique.

Table 7
Wave Boundary Layer Bottom Shear Formulae

Form/ Author	Formulae	Definitions	Comments
1.) Jonsson (1963)	$\tau_{bm} = \frac{.0604}{\log \frac{30 \delta \omega T}{k_s}}^2 \frac{\rho u_m^2}{2}$	$\delta \omega T$ = Turbulent wave boundary layer thickness; k_s = Nikvadsse sand roughness; u_m = maximum horizontal wave velocity; ρ = density; H_s = significant wave height; T_s = sig. wave period; d = depth; L_d = wavelength.	τ_{bm} = maximum instantaneous bottom shear. $u_m = \pi H_s / T_s \sinh [2\pi d / L_d]$
2.) Teleki (1972)	$\tau_b = \rho k_z \left(\frac{\partial u}{\partial z} \right)_{z=0}$	k_z = eddy viscosity; $k_z = k u_{*wm} z$; $k = V_{cn}$ Karmen's coefficient; u_{*wm} as in Eq. 1	τ_b = the time varying bottom shear. k_z is that due to Grant and Madsen (1979) and is steady during wave cycle. Evidence (Fredsoe 1984) is that constancy assumption is incorrect.
3.) Sheng and Lick (1979) Among others.	$\tau_b = 1/2 \rho f_w u_m^2 \cos \frac{2\pi t}{T_s}^2$	f_w = friction factor (Jonsson, Kamphuis, 1975)	Assumes sinusoidal waves; friction factors not well known for Lake Erie or any other site as they are too site and regime specific. Used for Lake Erie simulations.
4.) Fredsoe (1984)	Iteration procedure involving three equations.	Solves for the max shear and friction velocity in the wave boundary layer.	Formulae break down with presence high frequency waves because of turbulence memory effects.

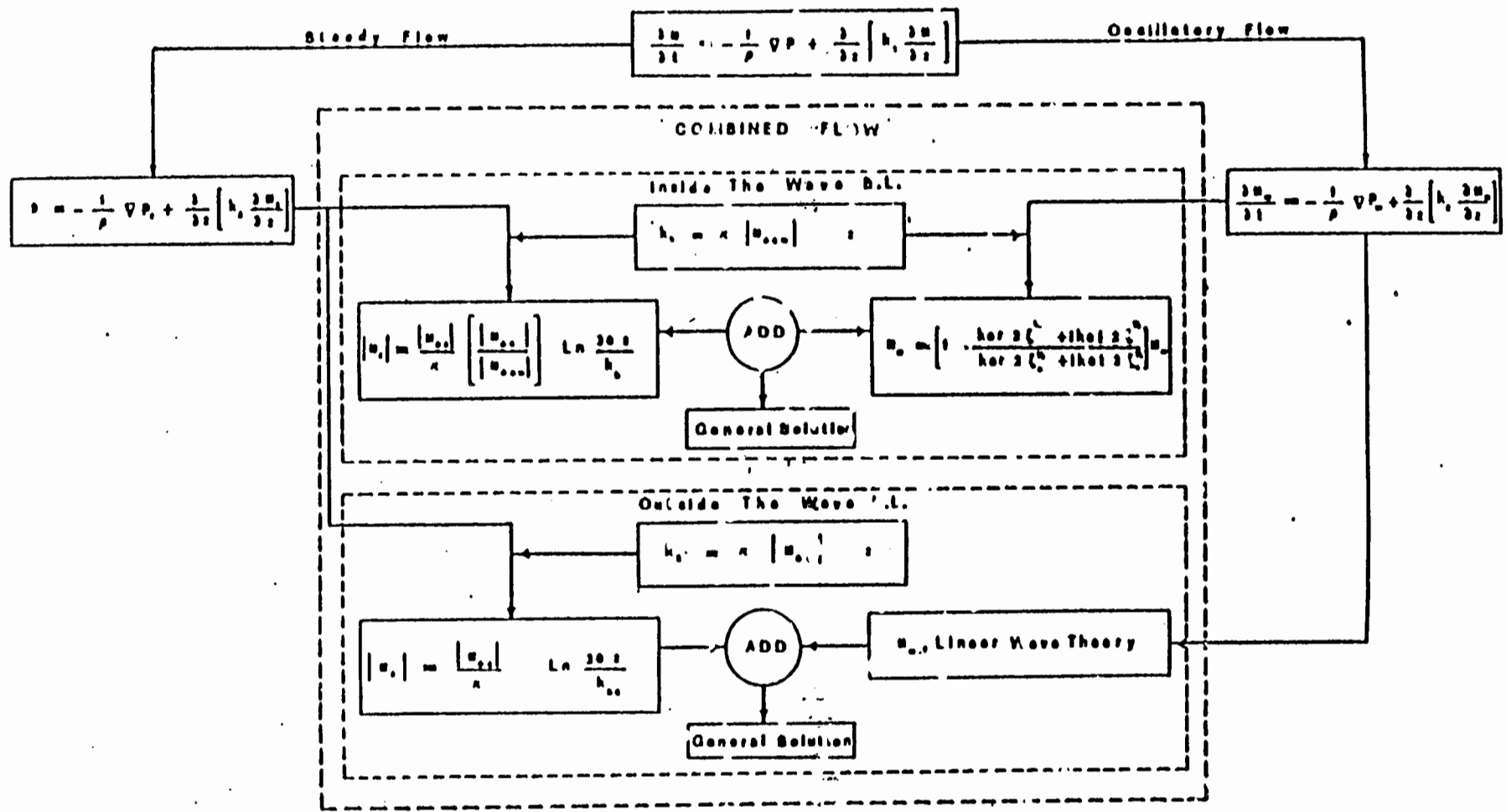


Table 4 A schematic diagram of the model presented by Grant and Madsen (1979) and Glenn (1983) for the flow kinematics. $\nabla = \partial/\partial x \mathbf{i} + \partial/\partial y \mathbf{j}$, $P = P_c + P_o$, $u = u_c + u_o$, $\xi = z/\lambda$, $\xi_o = z_o/\lambda$, $\lambda = \kappa |u_{c,0}|/\omega$, K_b is the bottom roughness, K_{bc} is the apparent bottom roughness.

Table 9 Critical Erosive Stress for Cohesive Sediments
(To Be Configured after W.Lick's Final Results)

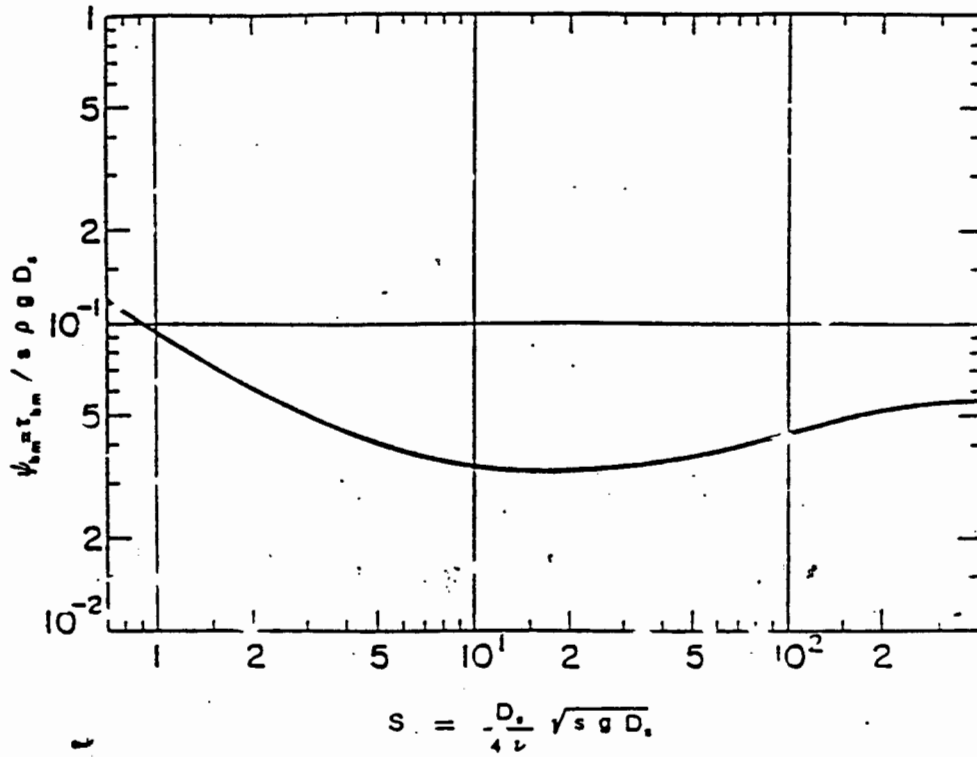


Table 10 Modified Shield's Diagram for Critical Erosive Stress of Non cohesive Sediments (Grant and Madsen, 1976)

Table 11

Trenton Channel Flow Extreme Value Analysis; Annual Interval
1971 - 1983 period of data record.

Return Interval (Years)	Duration - Averaging Interval				
	1 day	3 day	7 day	30 day	365 day
1.01	51942 (cfs)	50453	49842	48439	45581
1.05	53284	51270	50373	49469	46496
1.11	54101	51807	51467	50781	47049
1.25	55193	52565	52230	50781	47787
2.00	57632	54384	53834	52355	49421
5.00	60597	56772	55643	54159	51388
10.00	62387	58283	56677	55201	52564
25.00	64498	60119	57853	56395	53942
50.00	65983	61440	58654	57213	54905
100.0	67405	62726	59404	57983	55823
cv ¹	.057	.048	.038	.039	.044
σ^2	3299	2623	2049	2033	2190

1 coefficient of variation
2 standard deviation

Table 12

Trenton Channel One Year Risk Analysis
1971 - 1983 Period of Data Record

Return Interval, \bar{N} Years	Probability	Risk (R)
1.01	0.99	0.99
1.05	0.95	0.95
1.11	0.90	0.9
1.25	0.8	0.8
2.00	0.5	0.5
5.00	0.2	0.2
10.00	0.1	0.1
25.00	0.04	0.04
50.00	0.02	0.02
100.00	0.01	0.01

Table 13

North Wind Distributional Tests - Seasonal

Distribution	Season			
	Su:6/16-9/30	F:10/01-12/31	W:01/01-3/15	Sp: 3/16 - 6/15
Normal	moderate ³	poor	moderate ¹	poor ¹
Log Normal	poor	poor	poor	poor
Type I (fit/cv/R ²)	mod ⁴ /6.26/.97	good ⁴ /5.17/.99	mod ⁴ /5.17/.99	good/5.38/.98

- 1 Underestimates tails
- 2 Overestimates tails
- 3 low end discrepancy
- 4 high end discrepancy

cy - coefficient of variation
R² - correlation coefficient

Table 14

South Wind Distributional Tests - Seasonal

Distribution	Season (Table 12 for def)			
	Su	F	W	Sp
Normal	poor	good ¹	good ¹	poor
Log Normal	poor	poor	poor	poor
Type I (fit/cv/R ²)	good ⁴ /4.21/.99	good ⁴ /6.27/.98	mod ⁴ /6.49/.98	good/2.15/1.00

See Table 14 for definitions

Table 15

Temperature Distributional Tests - Seasonal

Distribution	Season (see Table 12)			
	Su	F	W	Sp
Normal	poor	good ²	good	moderate
Avg/Std. Dev.	68.8°F/7.05°F	39.7/12.8	25.8/11.2	52.0/13.0
LogNormal	poor	poor	poor	poor
Type I	poor	poor	poor	poor

See Table 14 for definitions

Pattern Analysis of North Wind Events - Monthly
(1973 - 1983 record years)

Month	Variable i) WIND SPEED ii) TEMPERATURE	No. of Events in Record	MEAN	MIN EVENT AVERAGE VALUE	MAX EVENT AVERAGE VALUE	AVG HOURS PER MONTH IN EVENT
JAN	Wind Speed (MPH) Air Temp (°F)	401	5.08 20.10	0.00 -9.00	18.00 43.00	36
FEB	"	497	6.47 21.91	0.00 -1.00	20.00 54.00	45
MARCH	"	534	6.17 31.0	0.00 0.00	25.00 57.00	48
APRIL	"	615	6.78 41.6	0.00 10.00	26.00 81.00	56
MAY	"	802	4.25 54.2	0.00 28.00	20.00 89.0	73
JUNE	"	727	3.24 67.4	0.00 47.00	18.00 92.00	62
JULY	"	866	3.6 67.4	0.00 47.00	19.00 92.00	79
AUG	"	914	3.6 66.5	0.00 40.00	19.00 91.00	84
SEPT	"	881	3.55 57.5	0.00 34.00	18.00 91.00	80
OCT	"	676	4.93 44.2	0.00 23.00	20.00 67.00	61
NOV	"	452	4.59 37.4	0.00 17.00	18.00 66.00	41
DEC	"	449	6.98 28.2	0.00 6.0	23.00 56.00	41

Table 17
 Pattern Analysis of South Wind Events - Monthly
 (1973 - 1983 record years)

Month	Variable i) WIND SPEED ii) TEMPERATURE	No. of Events in Record	MEAN	MIN EVENT AVERAGE VALUE	MAX EVENT AVERAGE VALUE	AVG HOURS PER MONTH IN EVENT
JAN	Wind Speed (MPH) Air Temp (°F)	359	9.60 27.15	2.00 -8.00	29.00 58.00	33.0
FEB		333	7.85 28.1	2.00 -5.00	20.00 59.00	30.5
MARCH		380	9.34 43.2	2.00 5.00	24.00 72.00	34.5
APRIL		381	9.2 53.7	2.00 26.00	26.00 82.00	35.0
MAY		462	7.82 62.9	1.00 36.00	22.00 91.00	42.0
JUNE		505	7.78 69.5	1.00 44.00	25.00 86.00	46.0
JULY		527	6.53 74.00	2.00 53.00	22.00 94.00	48.0
AUG		455	6.58 73.1	1.00 52.00	16.00 92.00	41.0
SEPT			6.92 65.33	2.00 34.00	16.00 87.00	43.5
OCT		535	8.44 55.8	1.00 25.00	21.00 80.00	48.5
NOV		443	8.94 46.5	2.00 17.00	24.00 75.00	40.0
DEC		395	8.52 32.3	2.00 0.00	22.00 67.00	36.0

Table 18
 Inter Event Time Pattern Analysis - Monthly
 (1973 - 1983 record years)

Month	South Events				North Events				All Events			
	No. Events	Mean Time (m)	Min Time (Hr.)	Max Time (Hr.)	No. Events	Mean Time (Hr.)	Min Time (Hr.)	Max Time (Hr.)	No. Events	Mean Time (Hr.)	Min Time (Hr.)	Max Time (Hr.)
Jan	187	43.7	1.00	441.0	219	39.7	1.00	287.0				
Feb	186	40.7	1.00	242.0	265	34.0	1.00	218.0				
March	219	39.9	1.00	326.0	281	34.4	1.00	221.0				
April	228	38.9	1.00	219.0	328	32.8	1.00	276.0				
May	304	35.4	1.00	259.0	436	28.5	1.00	192.0				
June	317	31.5	1.00	210.0	396	29.2	1.00	326.0				
July	367	30.9	1.00	250.0	485	26.6	1.00	284.0				
Aug	300	35.3	1.00	253.0	519	26.7	1.00	226.0				
Sept	301	35.7	1.00	218.0	465	27.1	1.00	188.0				
Oct	263	36.9	1.00	227.0	380	30.8	1.00	288.0				
Nov	231	39.3	1.00	379.0	256	36.0	1.00	320.0				
Dec	233	41.8	1.00	307.0	240	40.1	1.00	433.0				

Table 19

Summary of Trenton Channel Entrainment Deployments

Station No.	Station Name/Location	Depth (m)	Water Temp (oc)	Duration of Record	Comments
25 A.	Hennepin Point	7.6	13	50 minutes	Sandy Bottom; strong currents
CHT#1	Chen Han Tsai #1	5.5	13.5	3 hr. 4 min	Moderate current, building waves
NA	Gibraltar Channel	5.1	13.	1 hour	
54E	Mouth of Gibraltar Bay	4.6	13	1 hr. 5 min.	Sand bottom; strong current